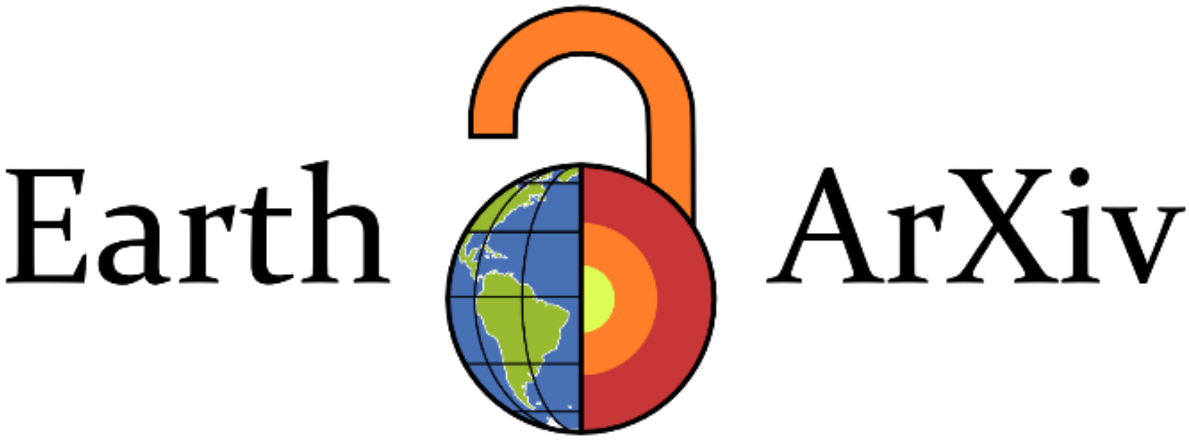

van Hinsbergen, D.J.J., and Wu, J., submitted, Chapter 13: Tectonic reconstruction. In: Webb, A.A.R., Briggs, S.M., Ganbat, A., Genge, M.C., and Moore, W.B. (eds), Methods in Tectonics. Geological Society, London, Geoscience in Practice.

Tectonic reconstruction

Douwe J.J. van Hinsbergen[1], Jonny Wu[2]

1. Department of Earth Sciences, Utrecht University, Princetonlaan 8A, 3584 CB Utrecht, the Netherlands

2. Department of Geosciences, University of Arizona, Tucson, Arizona 85721, USA

13.1 Introduction

Tectonic reconstruction is the process of *recreating how modern geological units have moved relative to one another through time and space*. The detailed studies in field mapping and measurements, and laboratory analyses summarized in previous chapters leave the geoscientist with the tools to reconstruct the tectonic history from today's geological architecture. Tectonic reconstruction is the core element of tectonic synthesis: larger-scale plate tectonic reconstructions provide boundary conditions for detailed analyses of regional tectonic systems whereas regional-scale tectonic analysis provides constraints for the broader tectonic setting. Tectonic reconstructions that describe the movement of geological units through time and space help to transform qualitative geological observations into quantitative kinematic models, providing a mathematical bridge between natural geological observations and the underlying physical drivers (Fig. 13.1). Tectonic reconstructions also provide valuable insights for researchers in other geoscientific fields because the former positions of geological units help us to contextualize and understand many processes that occurred in the geological past. For instance, the reconstruction of a fold-and-thrust belt impacts the understanding of paleogeography (i.e. historical landscapes). This may provide independent insight for scholars seeking to understand evolutionary biology or paleoclimate. For other terrestrial

planets and the earliest Earth, reconstruction is a critical tool by which we attempt to understand past tectonic modes that are far less well resolved compared to modern plate tectonics.

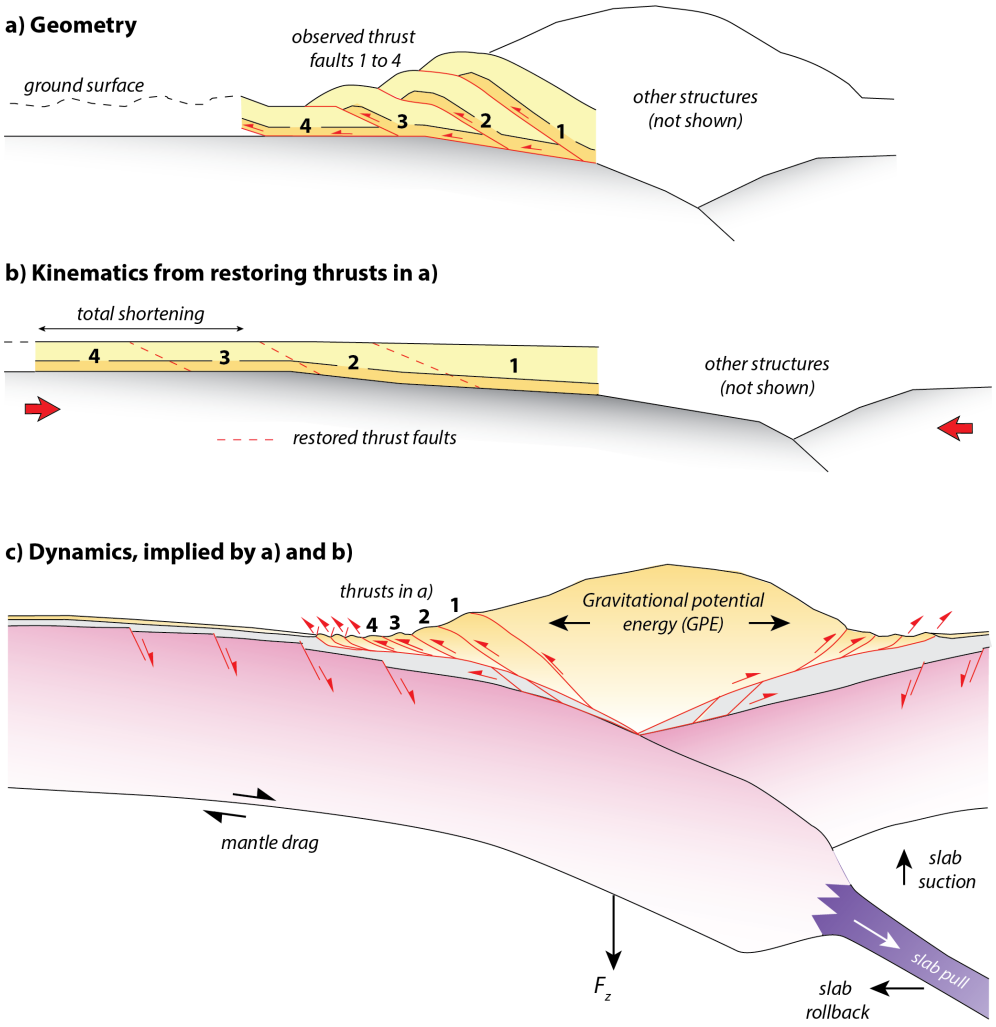

Figure 13.1: Cartoon cross-sections showing links between structural geometries, kinematic history, and implied dynamics. In a), recognition of the thrust 1 to 4 geometries allows kinematics to be inferred from a structural restoration in b). Kinematic histories from tectonic reconstructions such as b) can be used to infer geodynamics in c).

13.1.1 Key challenges

The **inherent incompleteness of the geologic record** can be appreciated from the classic angular unconformity exposed at Praia do Telheiro, SW Portugal (Fig. 13.2), which shows tens of million years of missing geologic time during formation, erosion, and breakup of the supercontinent Pangea. Given these challenges, the geologist must **navigate and reconcile a sheer diversity of tectonic constraints** (i.e. see other chapters in this book) when making a tectonic reconstruction that offer very different perspectives on a geological history, but that are all relevant. Field-based information to understand orogenesis comes from stratigraphy, sedimentology, paleontology, structure, metamorphism, magmatism, geochronology, geochemistry, paleomagnetism, and stable isotopes. Each of these sources of information is relevant but in isolation, none of them provide the full tectonic history. The perspectives from specialized communities have in the past proven difficult to reconcile on the scale of the ultimate plate tectonic and paleogeographic reconstruction. Instead, we will discuss ways to integrate such data at a smaller scale, and in an earlier, less controversial step of the reconstruction procedure, to overcome such difficulties.

13.1.2 Chapter scope

There are numerous geological phenomena that may be reconstructed, but in this chapter, we focus on the reconstruction of tectonic motions at intraplate and accretionary orogens. Intraplate orogens form by deformation (shortening) of a lithosphere, often reactivating earlier zones of weakness such as rifts or old sutures. They typically have relatively low magnitudes of displacement - 10's to a few 100 km of convergence - but make major orographic barriers that are key to reconstruct paleogeography. Accretionary orogens are the sole geological record of the vast geological infrastructure that Earth has recycled through subduction throughout its billions of years of plate tectonics. Accretion is the tectonic process during which rock units transfer from a subducting to an overriding plate and thus become the scarce geological remains that escape subduction. We will

discuss how we may use such geological records to inform about the paleogeographic distributions and properties of oceanic and continental lithosphere that was lost to subduction, and the tectonic plates and their motions that existed therein.

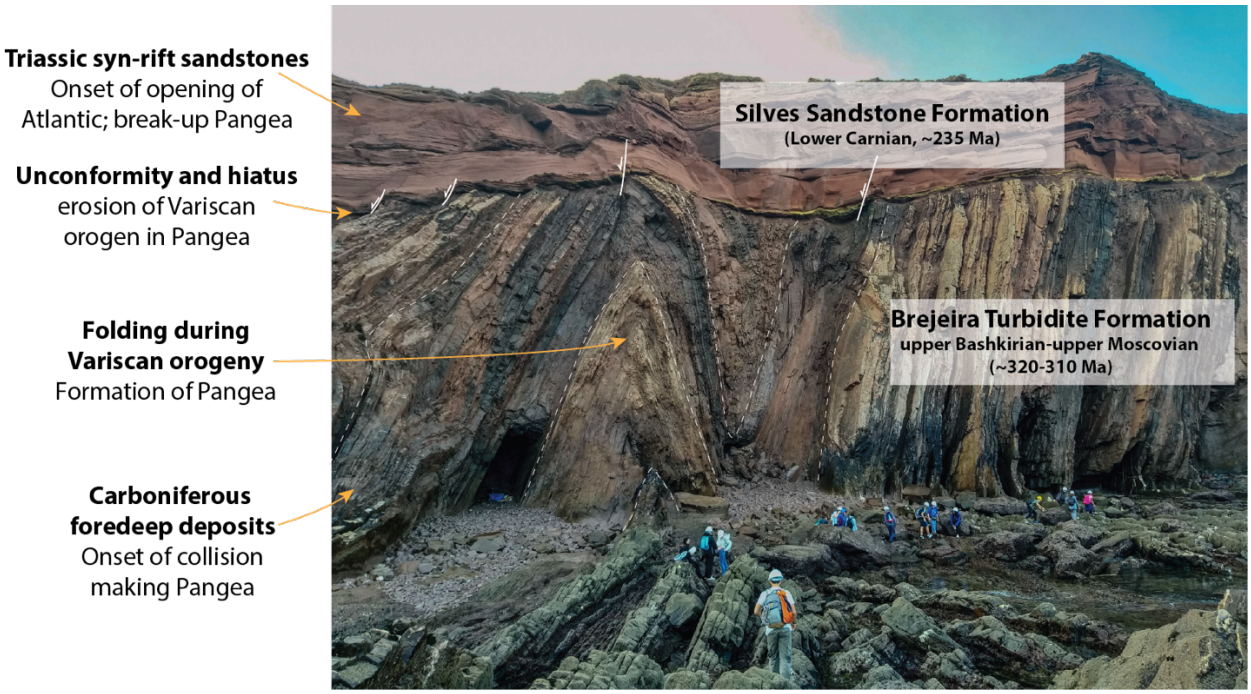

Figure 13.2: Cliff section of Praia do Telheiro, SW Portugal, showing in one exposure the geological remnants of formation, erosion, and break-up of the supercontinent Pangea. The angular unconformity between the overlying, sub-horizontal Silves sandstone and underlying, folded and deformed Brejeira turbidites indicates 75 to 85 million years of missing geologic record. Photo courtesy of Joao Duarte, University of Lisbon, Portugal.

From the perspective of a field geologist, we will discuss the reconstruction of horizontal tectonic motions, both from regional field observations of intraplate deformation, as well as from global plate tectonic reconstructions. We will illustrate how the difference between these perspectives from different length scales may inform the maker of paleogeographic areas that were lost to tectonic burial through time, especially through

subduction. We will describe the mechanisms by which we may reconstruct deformation in a reproducible way, weighting and integrating independent analysis techniques that may include marine geophysics, structural geology, stratigraphy and sedimentology, metamorphism and magmatism, geochemistry, paleomagnetism, and seismic tomography.

13.2 Kinematic reconstructions

Kinematic reconstructions restore modern geological records to their undeformed state based on quantified tectonic motions, or the 'kinematics' (Fig. 13.1b). The benefit of 'kinematics' is that the maker of the reconstruction does not need to understand the set of forces that *cause* and resist the motions, or the 'dynamics': kinematics constrain dynamics (Fig. 13.1c). For instance, plate tectonics is a kinematic concept: one may understand how plates move without understanding the geodynamics that drive such motions, but not vice versa.

The starting point of such a kinematic reconstruction is typically a series of field observations (e.g. from a mapping project) but a major difficulty for the field geologist is the lack of detailed kinematic knowledge outside of the mapping area. An effective way to place detailed local field knowledge into a global and regional kinematic context is to use paleo-GIS software such as the free plate reconstruction software GPlates (https://www.gplates.org/) (Müller *et al.* 2018). Examples of tectonic reconstructions that can be viewed in GPlates include both global-scale (e.g., Seton *et al.* 2012; Torsvik and Cocks 2017; Müller *et al.* 2019) or regional-scale studies (e.g., van Hinsbergen *et al.* 2020b; van de Lagemaat and van Hinsbergen 2024). Adding field observations into a plate tectonic reconstruction often offers a way to evaluate the impact of the new findings and to identify key new research questions for the field.

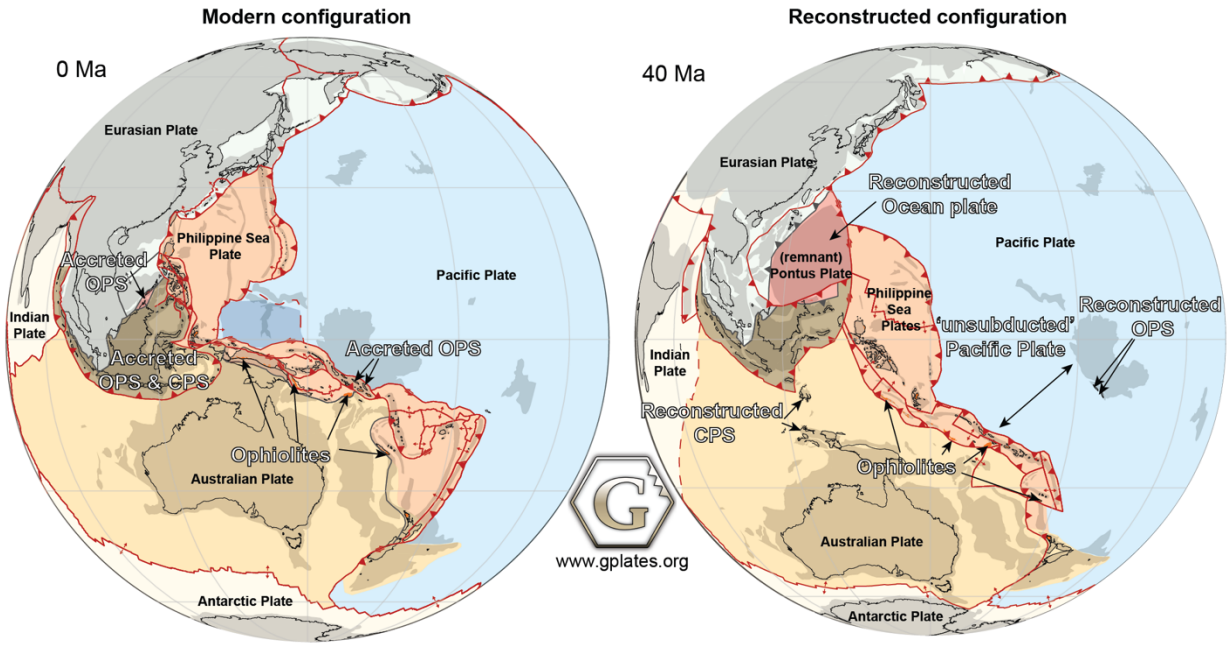

Figure 13.3: Example of a tectonic reconstruction in map view, of accretionary orogens in SE Asia of Advokaat and van Hinsbergen (2024) for circum-Indonesia and van de Lagemaat and van Hinsbergen (2024) for the circum-Philippine Sea Plate region, made with GPlates plate reconstruction software (Müller *et al.* 2018). Elements recognized in modern orogenic belts (left panel), such as ophiolites, accreted ocean plate stratigraphy (OPS) or continental plate stratigraphy (CPS) are reconstructed to the positions on the plates they were derived from (right panel). Figure modified from van de Lagemaat and van Hinsbergen (2024).

TOP TIPS ZOOM OUT BOX HERE *(*60 words with 22 character heading) text below is 157 words, need to shorten)*:*

GPlates software: In the last two decades, GPlates plate reconstruction software (Fig. 13.3) has become a community standard. The software, largely developed and maintained by the EarthByte group of the University of Sidney (Müller et al. 2018) describes the relative motion between polygons, line

features, or point features, as rotations around Euler poles, as has been done since the birth of the theory of plate tectonics (McKenzie and Parker 1967). Relative rigid block rotations may be described by rotations of polygons, whereas intraplate deformation may be approximated by relative motions between line features, leading to changing areas that reflect distributed strain (van Hinsbergen and Schmid 2012; Müller et al. 2019). Global reconstructions are now available by different authors (e.g., Torsvik and Cocks 2017; Merdith et al. 2021) and underlie tools for paleoclimatologists (e.g., paleolatitude.org (van Hinsbergen et al. 2015a)) and paleobiologists (Buffan et al. 2023). Such reconstructions thus allow to translate the impact of detailed tectonic analysis to a multidisciplinary audience.

The current state of the art of global relative plate and orogenic tectonic reconstructions are a combination of three reconstruction approaches (Boschman *et al.* 2014; van Hinsbergen *et al.* 2015a; Seton *et al.* 2023). First, global scale reconstructions of relative plate motions are made following the paradigm of plate tectonics that the Earth's lithosphere is broken into rigid plates that move along discrete plate boundaries (see Sec. 13.2.1). Second, regional scale reconstructions focus on the regions where this paradigm fails: intraplate deformation belts - both close to active plate boundaries or far away - where plates are not rigid, but deforming (see Sec. 14.2.2; Fig. 14.7). Such **distributed intraplate deformation** may be extensional such as the East African Rift (Macgregor 2015) or the Basin and Range province (McQuarrie and Wernicke 2005), strike-slip dominated such as in the Gobi and Mongolian Altai or on Jamaica and Hispaniola (Cunningham and Mann 2007), or contractional, such as the Andes (DeCelles and Horton 2003) or the Sevier and Laramide belts of the western USA (Yonkee and Weil 2015), or the Tibetan Plateau (Yin and Harrison 2000; Kapp and DeCelles 2019). Figure 14.7 shows an example of intraplate deformation from geodesy of the western USA Cordillera. Here, various intraplate deformation styles (i.e. strike-slip, extension and contraction) are occurring

simultaneously. Combined, these reconstructions reveal how the geological units exposed at the Earth's surface have moved relative to each other over geological time.

Third, incomplete, and often **sparse accreted remains of subducted lithosphere** (see Sec. 14.3) may be used to reconstruct the plates, and their paleogeography, that have been recycled into the mantle. These plate reconstruction elements are explained in detail below. Finally, to use these relative plate reconstructions to decipher the earth system processes, they need to be placed in a **reference frame** (Sec. 14.4), either relative to Earth's spin axis for paleo-climatic or -biological problems, or relative to the mantle for geodynamic problems, which we will briefly address at the end of the chapter.

14.2.1. Relative plate motions: rigid plate reconstructions and plate motion chains and circuits

The most accurate reconstructions of relative plate motions are based on marine geophysical datasets from the modern oceans. Magnetic stripes of the sea floor that represent magnetic reversals recorded in basaltic ocean floor during oceanic spreading are mirrored in mid-oceanic ridges (Vine and Matthews 1963) and show that spreading is typically (although not always (Müller *et al.* 1998)) near-symmetric. This process of spreading is observable on the meter scale in the field, in sheeted dike complexes of 'ophiolites': exposed fragments of oceanic crust. The parallel, 'sheeted' basaltic dikes, typically 0.5-1.5 m thick, are interpreted to have intruded, following a spreading pulse, at the spreading ridge axis where the ophiolitic crust formed (Anonymous 1972). But of most of such dikes only one side reveal a chilled margin that forms when magma of the dike intruded and became juxtaposed against cold wall rock. Such a chilled margin must also have formed on the other side of the dike, but is not exposed: instead, the dikes coarsen away from the chilled margin, suggesting cooling was slower, and are then abruptly juxtaposed against the chilled margin of the next dike (e.g., Robinson *et al.* 2008; Phillips-Lander and Dilek 2009). This means that sheeted dike sequences only contain 'half-dikes'; the other half of the dikes became part of the plate that spread away from the crust of the

ophiolite. Sheeted dikes show on the field scale why magnetic anomalies are mirrored in mid-oceanic ridges (Fig. 14.4).

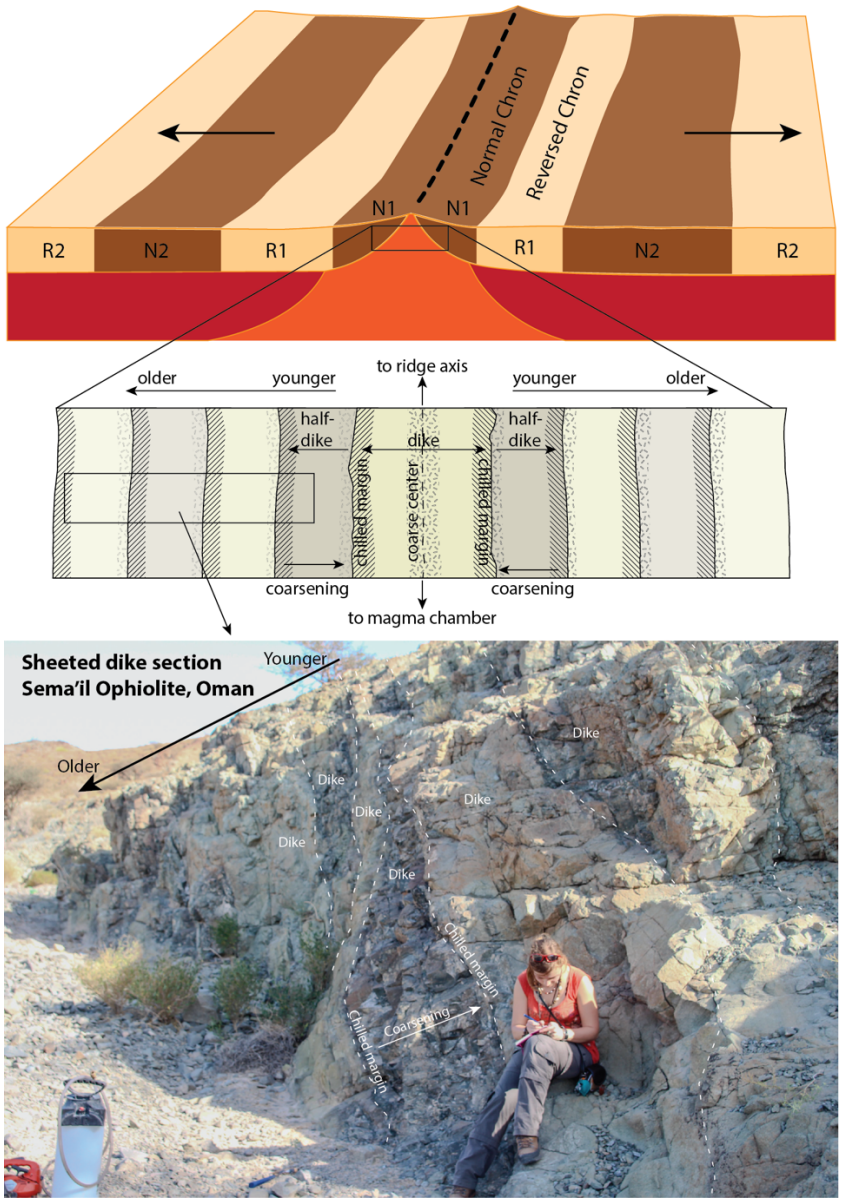

Figure 14.4: Relationship between sheeted dike sections and near-symmetric spreading at mid-oceanic ridges. Upon spreading, dikes fracture in the coarse-grained center, accreting one half to each plate, and with intrusion of the younger dike in the center of the older.

The width of the anomalies and the magnetic polarity timescale that provides ages of the reversals (Gradstein *et al.* 2020) together constrain the rate at which spreading occurred (Vine and Matthews 1963). Transform faults and fracture zones then provide the spreading direction (Figure 14.5).

Plate motions on a sphere are described by rotations around Euler poles: the transform faults and fracture zones provide the small circles around the Euler pole and the magnetic anomalies form parallel to great circles through the pole (Figure 14.5) (McKenzie and Parker 1967; Cox and Hart 1986). Legacy data typically came without uncertainty estimates, but modern reconstructions quantify Euler pole uncertainty matrices, and these can be propagated to quantify uncertainty in relative plate motion (Doubrovine and Tarduno 2008).

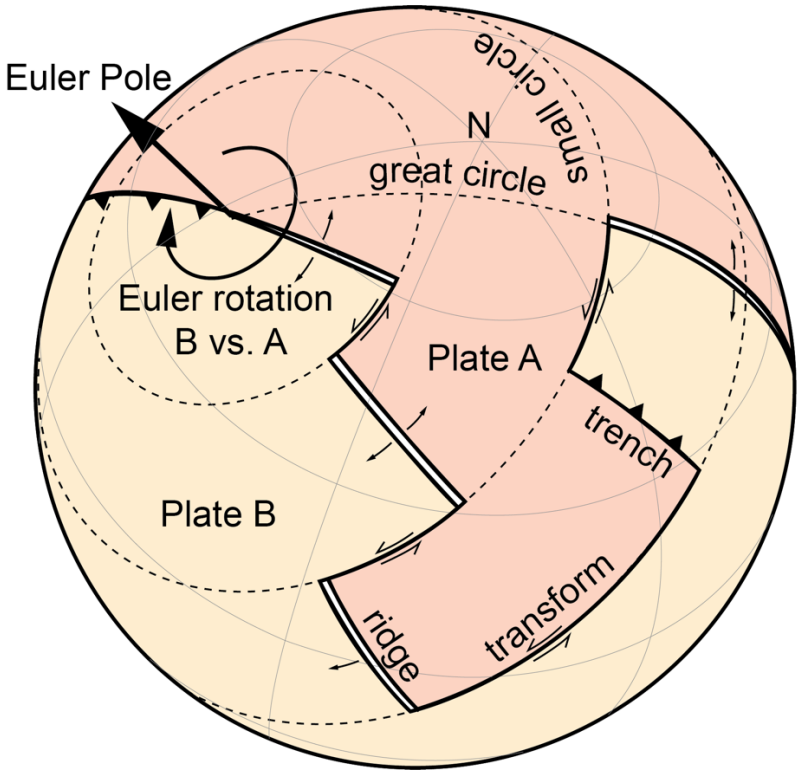

Figure 14.5 Relative motion between two plates on a sphere are described as rotations around Euler poles, with a geographic location (described as latitude, longitude) and a rotation of one plate versus another in a given time window.

This way, ocean basin reconstructions demonstrate the *relative motions* between the two conjugate plates. When multiple plates are connected through multiple mid-ocean ridges, *plate motion chains* (Fig. 14.6) may be established that describe a set of relative plate motions. For instance, the present-day relative motion between South American (SA) and Indian (IN) plates in Figure 14.6 can be reconstructed by the following plate motion chain: 1) South America (SA) to Antarctica (AN) via the American-Antarctic mid-ocean ridge; 2) Antarctica (AN) to Somalia (SO) via the SW Indian mid-ocean ridge; and, 3) Somalia (SO) to India (IN) via the Carlsberg ridge (Fig. 14.6). A plate motion chain that forms a complete loop that connects two converging plates across mid-ocean ridges is called a *plate circuit*. For example, the present-day North America-Juan de Fuca plate circuit is formed by connecting the following plates across active mid-ocean ridges (Fig. 13.6): North America (NA)-Africa (AF)-Antarctica (AN)-Pacific (PA)-Juan de Fuca (JF). When reconstructing the past motions of plates using plate motion chains, it is helpful to be aware that available mid-ocean ridge connections will vary over geologic time due to the finite lifespan of mid-ocean ridges (i.e. mid-ocean ridges will initiate and later become inactive).

The resolution of ocean basin reconstructions based on plate motion chains depends on the availability of magnetic reversals in the polarity timescale, which may vary from multiple per Myr to none for tens of Myr (e.g., the Cretaceous Quiet Zone, 125-83 Ma (Gradstein *et al.* 2020)). Moreover, most ocean basin reconstructions did not use every magnetic reversal on the sea floor but use selected reversals every ~5-10 Ma, assuming that changes in relative plate motion are gradual and slow. Recent detailed reconstructions for the Cenozoic have shown that this assumption is not always valid: particularly at high plate motions, rates may vary by 50% or more on short timescales of 1-2 Ma (DeMets and Merkouriev 2021), perhaps as a reflection of folding of rapidly subducting slabs in the upper mantle (van der Wiel *et al.* 2024b). Such rapid fluctuations may be tied to geological events, and increased ocean spreading resolution in future reconstructions may thus provide novel tectonic insight.

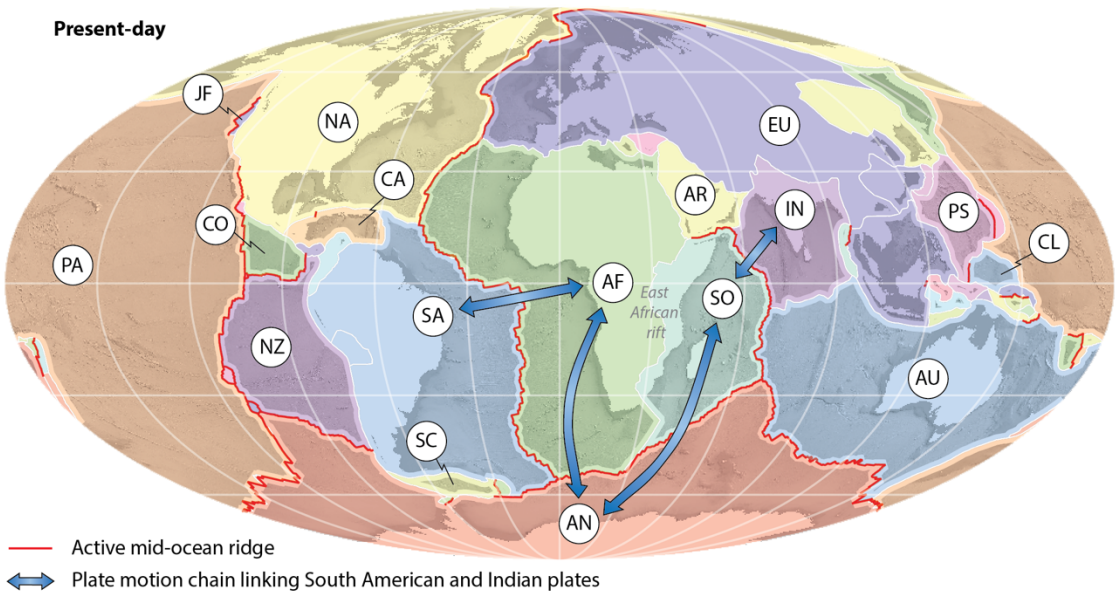

Figure 13.6: Map of Earth's present-day major tectonic plates (colored regions) simplified from (Bird 2003). Red lines show mid-ocean ridges. Blue arrows show a plate motion chain between the South America (SA) and India (IN) plates. Plate names: AF – Africa; AN - Antarctic; AR - Arabia; AU - Australia; CA - Caribbean; CL – Caroline; CO - Cocos; EU - Eurasia; IN - India; JF – Juan de Fuca; NA - North America; NZ - Nazca; PA - Pacific; PS - Philippine Sea; SA - South America; SC - Scotia; SO - Somalia; SU - Sundaland.

WORKED EXAMPLE 13.1: PLATE MOTION CHAINS

Using the map in Figure 13.6, determine the following present-day plate motion chains for:

a) relative motions between the Indian (IN) and Eurasian (EU) plates;
b) relative motions between the South America (SA) and Nazca (NZ) plates;
c) relative motion between Alaska and Siberia

On a sphere with constant volume, plate production by ocean spreading must be balanced by plate consumption, through subduction. Global reconstructions of the growth of modern oceans thus also quantify the area that must have been consumed, at still-active subduction zones, at former subduction zones now represented by sutures, and, for a small part, by intraplate shortening. If plates bordering active or former subduction zones are part of a plate motion chain, i.e., downgoing and overriding plate connected through former or active mid-ocean ridges, they form a *plate circuit*. These accurately quantify the rate of plate convergence through time and provide a well-constrained kinematic context for regional reconstructions of subduction-related tectonic deformation. For instance, convergence between India and Asia follows from reconstruction of the Eurasia-North America-Africa-India plate circuit (Fig. 13.6). Convergence rates across the Cascadian subduction zone of western North America follows the plate circuit from North America-Africa-Antarctica-Pacific-Juan de Fuca (Fig. 13.6) (whereby deformation of the West Antarctic Rift must be taken into account (Doubrovine and Tarduno 2008). In plate tectonic reconstructions, one plate is typically chosen as the root of a rotation tree, i.e., all other plates in a plate mosaic are eventually reconstructed relative to that root. The choice of that plate is arbitrary, but the default GPlates reconstructions use Africa as root, as Africa is surrounded by ridges that connect to many other plates (Fig. 13.6) (Seton *et al.* 2012; 2023).

The Pacific Plate - the largest tectonic plate on Earth, formed by spreading with a series of surrounding plates that have almost entirely been subducted. Even though those plates no longer exist, their formation and motion history, may still be estimated from magnetic anomalies that are preserved on the Pacific Plate (Engebretson *et al.* 1985). Such reconstructions, assuming that spreading was symmetric, provide useful context for the tectonic study of long-lived active margins. For example, in Japan and far east Asia, the subduction history of the conceptual Izanagi Plate that once occupied the NW Pacific realm is reconstructed from magnetic anomalies on the NW Pacific plate (e.g., Wu *et al.* 2022); the disappearance of the Farallon Plate below North and South America follows from anomalies on the eastern Pacific Plate (e.g., (onsdale 2005; Liu *et al.* 2008), and the

demise of the Phoenix Plate below Antarctica and New Zealand follows from anomalies in the Southern Pacific (e.g., van de Lagemaat *et al.* 2023).

Plate motion chains and plate circuits only exist for times from which oceanic crustal records remain, i.e. back to the break-up of Pangea, some 200 Ma ago. For older times, independent quantitative constraints on the relative motion of plates rely on paleomagnetic data from continents (see Chapter 12 (Fu and van Hinsbergen 2026)). Paleomagnetic data can constrain relative paleolatitudinal motions and vertical axis rotations between continents, as a proxy for relative plate motion, but not paleolongitudinal motions (e.g., Torsvik *et al.* 2012). As a result, pre-Mesozoic plate reconstructions, also when cast in GPlates context (e.g., Domeier and Torsvik 2014; Merdith *et al.* 2021) have much higher, and often unquantified uncertainty, even though they still provide context for tectonic interpretation.

13.2.2 Intraplate deformation

Intraplate deformation where the assumption of rigid plate behavior fails: Intra-plate deformation shows that plate tectonics is not only accommodated along discrete plate boundaries but is also distributed across deformation zones (Fig. 13.7). The total amount of cumulative displacement in those zones, and the rate and magnitude of displacement, is typically one or two orders of magnitude slower (mm/yr) than plate motions (1-10 cm/yr) (Kreemer *et al.* 2003; van Hinsbergen and Schouten 2021), and for understanding of global geodynamics, intraplate deformation is often ignored. For instance, the total amount of extension accommodated by rifting of 'typical' continental crust prior to the onset of oceanization is on the order of 150 km in each rifted margin (Torsvik *et al.* 2008). Continental extension in thickened orogenic crust may reach higher values (e.g., the Basin and Range province (McQuarrie and Wernicke 2005) and the Aegean region (van Hinsbergen and Schmid 2012) both underwent ~400 km of extension but oceanic conditions have not yet been reached). Nonetheless, these numbers are still dwarfed by the amount and rate of spreading of ocean basins. Likewise, intraplate shortening is

typically one or two orders or magnitude smaller than plate convergence. The largest known intraplate shortening for Phanerozoic orogens is in the Tibetan Plateau, ~1000 km (Replumaz and Tapponnier 2003; van Hinsbergen *et al.* 2011), and is mostly much less (up to ~400 km in the Andes (Eichelberger and McQuarrie 2015; Schepers *et al.* 2017), whereas plate circuits show that convergence in these regions accommodated by subduction was an order of magnitude larger (van Hinsbergen *et al.* 2011; Chen *et al.* 2019).

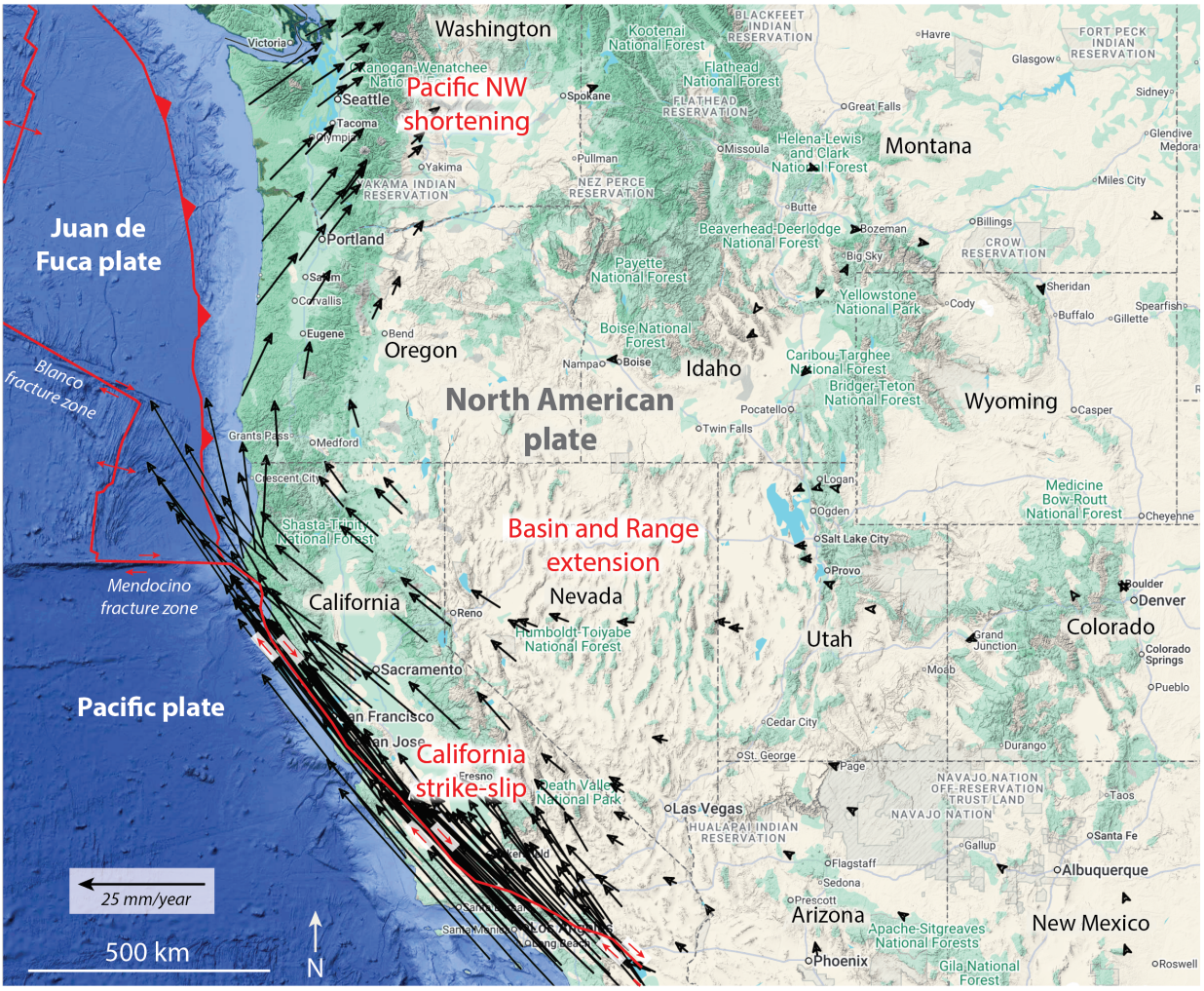

Figure 13.7: Map showing intra-plate deformation within western North America that includes shortening within the Pacific NW, extension within the Basin and Range, and strike-slip along California. Black arrows show tectonic motions measured by GPS relative to the stable North American plate interior to the east (Kreemer *et al.* 2014).

However, for development of topography and paleogeographic complexity, or for understanding earthquakes or economic geology, these zones of intraplate deformation are of paramount importance. Much of the attention of the geological community has focused on understanding the tectonic history of these intraplate deformation zones, where extension or erosion exhumed deep rock and associated resources. Associated shallow continental basins stored much of the hydrocarbon resources that have been used in the last century. And these belts with rich geographic diversity - in terms of islands and seaways in extensional regions, or steep ranges in contractional regions - form biodiversity hotspots.

The reconstruction of intraplate deformation is relatively straightforward, because in absence of major subduction zones that could remove geological infrastructure from the Earth's surface in its entirety, geological records may be fairly complete if surface exposure is sufficient. Reconstruction of the paleogeographic and tectonic evolution may thus rely on datasets that quantify motion, i.e. structural geology quantifying fault motion and paleomagnetism quantifying vertical axis rotation, cast in a geometrically consistent configuration within the wider context of reconstructed bounding-plate motions. In case of conflicting tectonic interpretations within an intraplate deformation region, the reconstructions may be made in a hierarchy (e.g., Boschman *et al.* 2014; van Hinsbergen *et al.* 2020b), ordered from most certain to least certain constraints on tectonic motion, as described below.

Structural geological records of intraplate deformation are the most complete for extensional terranes, because the maximum geological record is obtained at the end of an extensional tectonic event. Reconstruction of such extensional regions, in the form of rifts or metamorphic core complexes, may rely on estimates of fault displacement, crustal thinning or stretching factors, or simply the 're-burial' of an extensionally exhumed metamorphic terrain below its hanging wall (e.g., McQuarrie and Wernicke 2005). Next, reconstruction of intraplate strike-slip faults provides accurate information on relative

displacement direction, although the amount of fault displacement or its timing may be uncertain. Finally, shortening records only provide minimum estimates, because they leave the least complete geological record at the end of the tectonic event (e.g., Woodward *et al.* 1989).

Styles of intra-plate deformation

Importantly, on the scale of orogens, these three styles of deformation often occur in tandem (Fig. 13.8). Strike-slip faults typically connect at their tips to thrust belts or rifts, and thus different structural geological constraints may be used to reconstruct the undeformed geometry. For instance, the famous, left-lateral Altyn Tagh Fault of northern Tibet connects to the NE and SW with thrust belts that accommodate strike-slip fault displacement - estimated at some 400 km - through oblique shortening (Cowgill *et al.* 2003). Likewise, the transpressional orogens and basins of Mongolia and southeast Siberia are connected with strike-slip systems and their shortening and extension history must be consistent with the strike-slip fault displacements (Cunningham 2005).

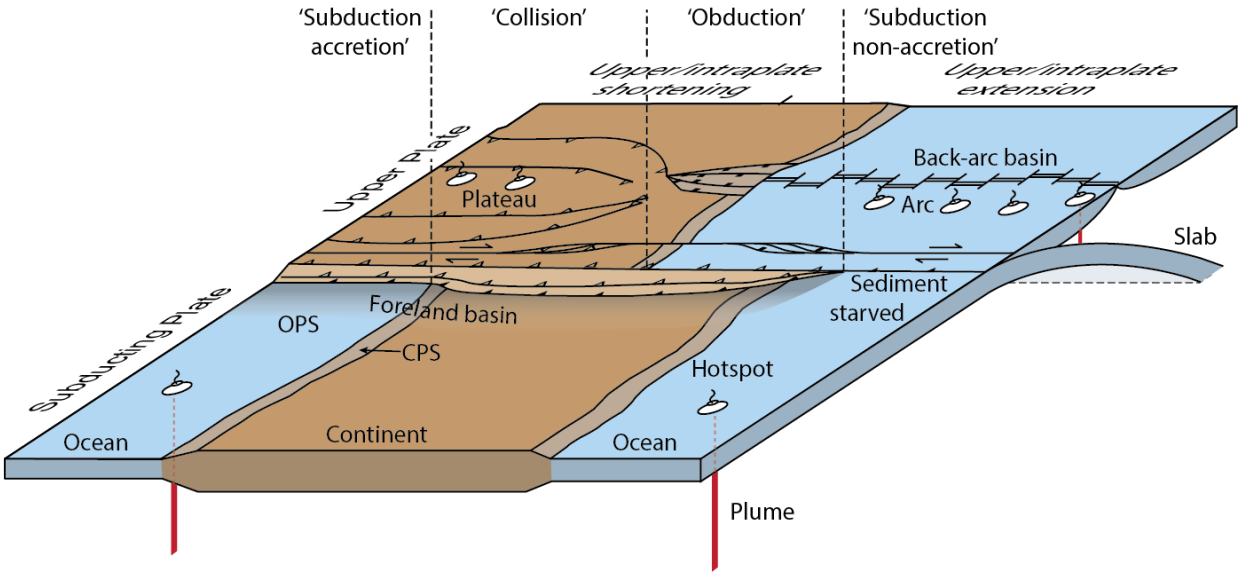

Figure 13.8: Cartoon showing styles of subduction, volcanism, and upper/intra-plate deformation. Modified from (van Hinsbergen and Schouten 2021).

Geometrical consistency is key for kinematic reconstruction: tectonic blocks cannot overlap in reconstructions unless there is evidence that they underwent extension, and they cannot contain space between if there is no evidence that they shortened. Moreover, intraplate deformation is, on orogen-scale, rarely cylindrical. More commonly, deformation reveals lateral gradients. For instance, shortening in the Tien Shan orogen in Central Asia is estimated to increase from zero in the northeast to ~200 km in the southwest (Yin *et al.* 1998). Extension in the Aegean region is ~400 km in the center but decreases to zero towards the northwest in the Balkans and east in western Turkey (van Hinsbergen and Schmid 2012). Lateral strain gradients equate to rotation differences around a vertical axis between rock units that bound the deforming belt. The lateral change in shortening in the Tien Shan requires a ~7° clockwise rotation of the Tarim Basin relative to Eurasia (Avouac *et al.* 1993). The lateral variation in extension in the Aegean region lead to a southward convex orocline with opposite rotations of western Greece and southwestern Turkey (Kissel and Laj 1988; van Hinsbergen and Schmid 2012). Paleomagnetic data may constrain such rotations, and, in combination with structural constraints, may allow reconstruction of the distribution of strain also for areas without detailed field data.

Paleomagnetic data also provide indications of total displacement in case deformation is dominated by strike-slip faults, particularly when those strike-slip faults reactivate former sutures, which hampers geological correlation. Such reactivations are common, e.g. in the North American Cordillera (e.g., Wyld *et al.* 2006) or in the West Burma Block (Westerweel *et al.* 2019). Such strike-slip displacements are often orogen-parallel and accommodate oblique plate convergence. Also in this case, much may be learned from the termination of the strike-slip faults, and with large displacements, these may result in widespread oroclinal bending and buckling. Hypothesized examples concern the New England orocline in eastern Australia that is thought to have accommodated margin-parallel translation of terranes along the east Gondwana margin (Cawood *et al.* 2011), or the Alaskan orocline accommodating northward translation of terranes along the western North American margin (Johnston 2001). Finally, paleomagnetically determined vertical axis rotations of

poorly exposed fault blocks in the jungle of the Yunnan region in Indochina explained how estimates of major block extrusion from SE Tibet - with fault displacements estimated at 700 km or more (Leloup *et al.* 1995) - could be reconciled with much smaller displacements of no more than ~300 km along the Red River Fault towards the southeast (Searle 2006; Fyhn *et al.* 2010) through internal deformation and rotation (Li *et al.* 2017).

The hierarchy described above for intraplate deformation works well for continental interiors and margins alike, and even for deformed modern oceanic plate interiors such as the Caribbean plate (Montheil *et al.* 2025). However, reconstructing lithosphere that was lost to subduction - mostly oceanic but sometimes also continental - is more challenging. Approaches to do so are explained below.

13.2.3 Reconstructing oceanic upper plate lithosphere using ophiolites

Remains of oceanic lithosphere are recognized in the geological record as ocean plate stratigraphy (OPS) (Isozaki *et al.* 1990), offscraped from subducted oceanic crust (see below), and as 'ophiolites'. Ophiolites are exposed remnants of oceanic lithosphere (Fig. 13.9) (e.g., Dewey 1976). In the literature, offscraped OPS is also sometimes referred to as 'ophiolite' (e.g., the Calabrian 'ophiolite' units of southern Italy (Rossetti *et al.* 2004), but we here refer to ophiolites only as the more or less coherent oceanic lithospheric units that include their mantle section, and that are widely recognized as remains of the leading edge of overriding oceanic lithosphere above (former) subduction zones (*cf.* Dewey and Casey 2011).

Modern examples of such leading edges of overriding plate oceanic lithosphere include the Philippine Sea Plate that sits above to the Pacific Plate at the Izu Bonin-Mariana subduction zone, or the eastern Caribbean plate that sits above subducting Atlantic Ocean crust attached to the North and South American Plate. The ultimate preservation potential of the Philippine Sea and Caribbean plates in the geological record is slim: both plates are already subducting, the Philippine Sea Plate at the Nankai subduction zone below SW Japan, and the Caribbean Plate at the Maracaibo subduction zone below Colombia.

However, their leading edges above subduction zones may get uplifted above accretionary prisms, or underthrusting continental margins, and in that case, they may become preserved in orogenic records, where they form an invaluable source of information for tectonic reconstructions.

The most famous of such upper plate ophiolites are the Troodos ophiolite of Cyprus and the Sema'il Ophiolite of Oman (Fig. 13.9), which have been instrumental in identifying the most complete (although typically still strongly attenuated) sequence of oceanic lithosphere: the Penrose sequence (Anonymous 1972). This sequence describes ophiolites from top to bottom as containing oceanic pelagic sediments that rained down on the ocean floor, pillow lavas that flowed out from the spreading ridge, sheeted dikes that fed those pillows, isotropic and layered gabbros that represented the magma chamber below the dikes and the cumulates that formed at the base of that chamber, respectively, and a depleted mantle section consisting of harzburgites and dunites from which the crustal magmas were derived by partial melting (Fig. 13.9). Where exposed above sea level, such ophiolites are almost always underlain by subduction-related accretionary orogens, often including a continental margin. Such accretionary orogens, discussed in detail in the next section, consist of crustal units, and the base of the ophiolite thus places mantle rock over crustal rock - a process that requires subduction.

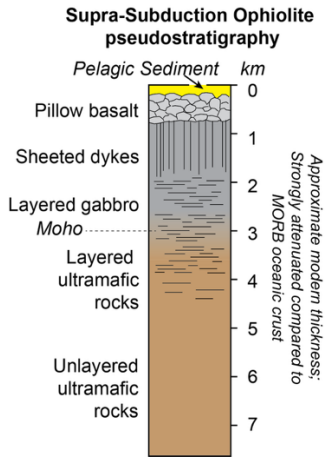

Figure 13.9: Cross-section showing a typical supra-subduction ophiolite sequence (pseudostratigraphy).

The geological jargon for the emplacement of ophiolites over continental margins is 'ophiolite obduction' (Dewey 1976) as opposed to 'subduction' that is the default behavior for oceanic lithosphere. However, this term is slightly misleading: it suggests that the ophiolite is undergoing some process to jump out of the ocean and onto the land. For tectonic reconstructions, it is better to view the process from a downgoing plate perspective: if subducting oceanic crust is attached to a passive continental margin, this margin will sooner or later arrive in the subduction zone and be dragged down below the upper plate (Fig. 13.10). If the forearc of that upper plate is oceanic, this brings oceanic lithosphere over continental crust. The arrival of continental margins in subduction zones often leads to slab break-off, after which the underthrust margin rebounds, uplifting the overthrusted oceanic forearc that then becomes exposed as ophiolite (Fig. 13.10). Alternatively, ophiolites may simply become uplifted because of accretion of buoyant nappes below the oceanic forearc, either ocean-derived (e.g., below the Californian or Andaman ophiolites (Wakabayashi 2015; Bandyopadhyay *et al.* 2020)) or continent-derived (e.g., in Anatolia (van Hinsbergen *et al.* 2016)). This way, the Sema'il Ophiolite of Oman was emplaced over ~180 km of the Arabian passive continental margin, of which ~50 km is currently exposed on land (McQuarrie and van Hinsbergen 2013). Reconstructed widths of the obducted forearcs of the West-Vardar Ophiolites of the Balkan, and the Cretaceous Neotethyan ophiolites of Anatolia yield restored widths of ~200 km (van Hinsbergen *et al.* 2020b).

However eroded, tectonically dismembered, or deformed, the structure, geochemistry, and age of ophiolites provide key information about subduction history and paleogeography. Following the plate tectonic revolution, ophiolites were originally interpreted as remnants of ocean floor that formed at regular mid-ocean ridges (Anonymous 1972). However, geochemical analysis soon revealed that most ophiolites found in orogenic belts formed by spreading above and close to a subduction zone (Miyashiro 1973), i.e. in the forearc. Those are known as 'supra-subduction zone' ophiolites (Casey and Dewey 1984; Pearce *et al.* 1984) and those proved much more common than true 'mid-ocean ridge basalt' (MORB) ophiolitic crust that formed prior to subduction

initiation - rare examples of those include the Masirah Ophiolite of eastern Oman (Peters and Mercolli 1998) or in a strip between the paleo-trench and SSZ oceanic crust in the west-Vardar ophiolites of the Balkan (Bortolotti *et al.* 2013) (Figure 13.10).

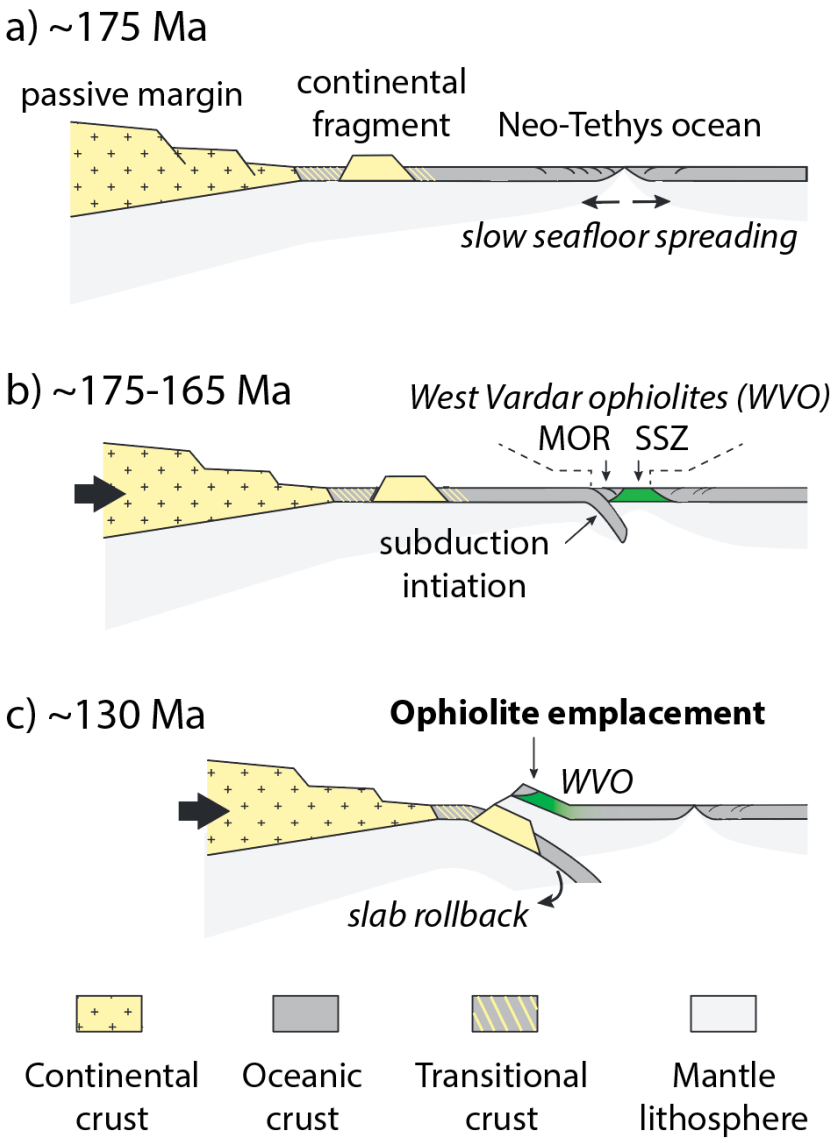

Figure 13.10: Example of ophiolite emplacement above a passive continental margin within the Neo-Tethys Ocean during the Mesozoic. The underthrust continental margin is buoyant and uplifts the overthrusted oceanic forearc, which then becomes exposed as an ophiolite (after Maffione and van Hinsbergen 2018)).

Stern and Bloomer (1992) and Stern *et al.* (2012) showed that the geochemical stratigraphy of SSZ ophiolites is well explained by a scenario of rapid extension in a forearc above a young subduction zone. This could then be explained by the onset of slab pull of a young slab, causing a catastrophic roll-back (Hall *et al.* 2003; Leng and Gurnis 2011), following a phase of induced convergence driven by far-field forces (Guilmette *et al.* 2018; 2023). A modern example of SSZ forearc crust that is still below sea level is the Izu-Bonin-Marianas forearc (Stern *et al.* 2012; Reagan *et al.* 2013), where forearc collapse occurred in the early Eocene following Paleocene subduction initiation along an intra-oceanic transform fault (van de Lagemaat and van Hinsbergen 2024). There are still many outstanding questions about the subduction initiation process - for instance, certainly not every subduction initiation process caused SSZ ophiolite formation (Lallemand and Arcay 2021), but SSZ ophiolites do form in any setting of subduction initiation: apart from the intra-oceanic transform fault as in the Izu Bonin-Marianas case, they were tied to subduction initiation along a mid-oceanic ridge in the Balkan Neotethys (Maffione *et al.* 2015), along a continental margin of the Pontides in Turkey, or southern Tibet (Topuz *et al.* 2014; Guilmette *et al.* 2023), in a back-arc basin in Cuba (Lázaro *et al.* 2013), or in an arc following arc-continent collision such as in the Andaman Islands (Plunder *et al.* 2020).

Besides marking the location of a former incipient subduction plate contact in an orogen, and offering insight into the timing of subduction initiation, ophiolites also provide quantitative constraints on the direction of oceanic spreading. Sheeted dike sections are thought to form parallel to spreading ridges (Fig. 13.4), and with paleomagnetic techniques, the original dike orientation may be quantified. To this end, dikes need to be restored to a vertical position, which is not a unique solution like tilting beds back to a paleohorizontal position - dikes tilted along an axis perpendicular to strike still renders the dike vertical. However, Allerton and Vine 1987) worked out a method to determine the options - through a 'net tectonic rotation' analysis, and through this method, paleo-spreading directions in ophiolites has been determined for many ophiolites (e.g., Inwood *et al.* 2009; Maffione *et al.* 2015; 2017). These prove remarkably coherent among ophiolites of the same age in the same belt (e.g., across the Neotethys (Maffione *et al.* 2017)) and allow

reconstruction of dismembered ancient plate boundaries to their original orientation. For instance, such an analysis suggested that the Jurassic ophiolites of California formed by ~N-S spreading, subparallel to and in the forearc of the paleo-trench, and the spreading rate could be estimated from the age distribution of the strongly dismembered and incomplete ophiolite remnants (Arkula *et al.* 2023). Hence, SSZ ophiolites are useful markers in the reconstruction of early subduction history and orogenic evolution.

13.2.4. Reconstructing tectonic deformation on other planets and moons

Even though Earth is the only planet we know of with plate tectonics, missions to other rocky planets, as well as rocky and icy moons in our solar system, show ample evidence that also their surfaces underwent tectonic deformation. The crust of Venus and Mars shows evidence for extension, folding, and thrusting (Nimmo and McKenzie 1998; Nimmo and Stevenson 2000; Golombek and Phillips 2010; Cascioli *et al.* 2025), likely related to gravitational collapse of topography as well as the cooling of the planet. The crust of Mercury, and of the Moon, has been shortened, likely due to cooling (Hauck II *et al.* 2004; Watters and Nimmo 2010; Man *et al.* 2023; Nahm *et al.* 2023). Complex deformation affected the crust of ice moons, such as Saturn's moon Enceladus (Yin and Pappalardo 2015; Schoenfeld and Yin 2024), or Jupiter's moon Europa (Collins *et al.* 2022). Those display a mosaic of small plates made of ice that moves relative to each other with strike-slip faults, normal rifts, and thrusts, likely driven by tidal forces.

Our understanding of the causes of deformation on these solar system bodies rests on very similar approaches that we summarized above for intraplate deformation on Earth. Image analysis helps to identify the mosaic of fault-bounded blocks, markers within neighboring blocks may identify displacement style and direction, and cross-cutting relationships provide relative timing. Such analyses invite kinematic reconstruction, such as in the example from Enceladus' South Polar region by Yin and Pappalardo (2015) in Fig. 13.11. Also for these analysis, GPlates plate reconstruction software may be used (Collins *et al.* 2022).

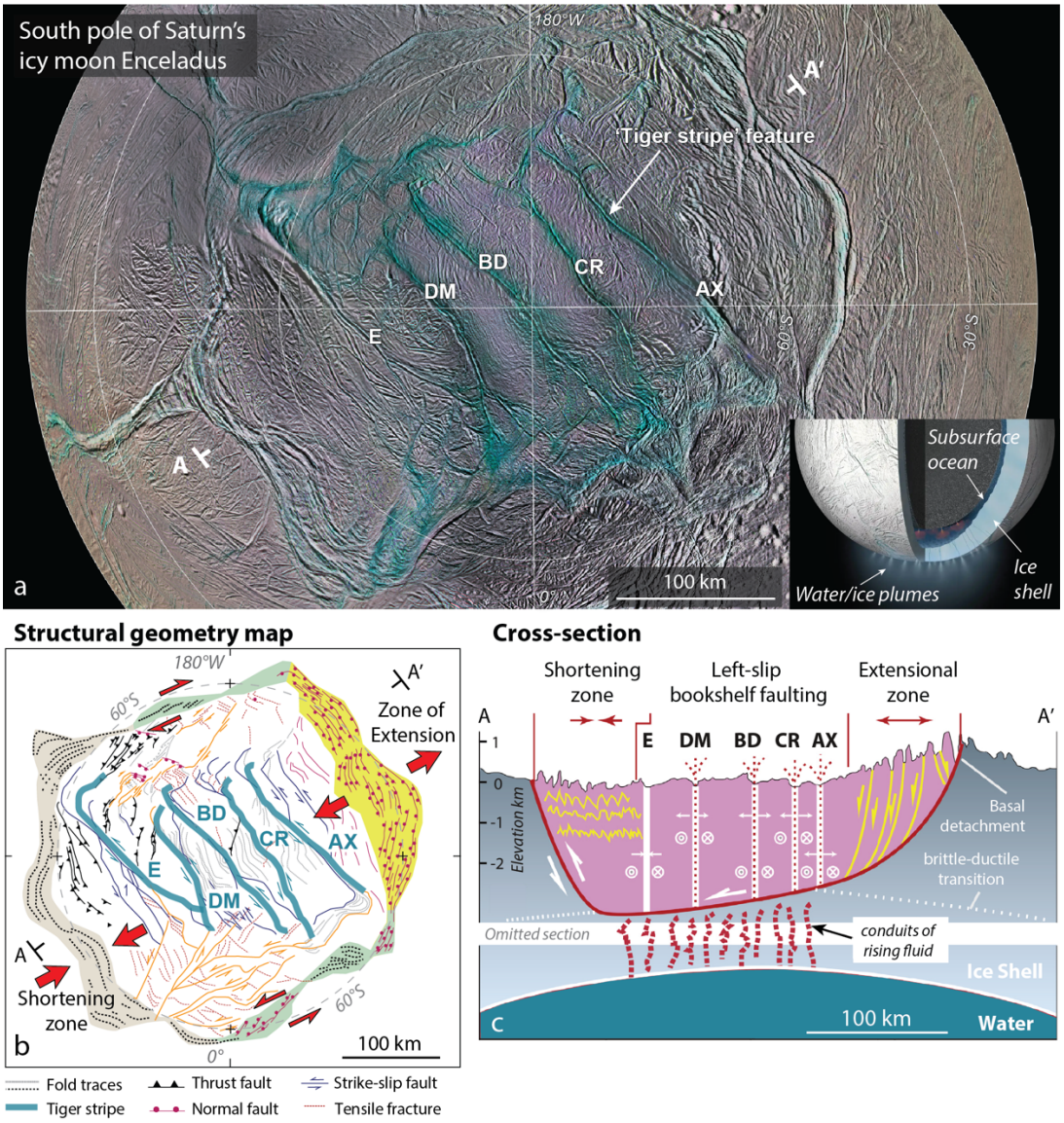

Fig. 13.11. a) False color map of the south pole of Enceladus, an icy moon of Saturn. Colored regions are highlighted by infrared and ultraviolet views that highlight 'tiger stripe' fractures where the moon's subsurface ocean vents icy vapor into space. Inset shows an artist rendition of Enceladus' interior that is formed by an icy shell above a subsurface ocean. Source: NASA. E, DM, BD, CR and AX denote the 'tiger stripe' features. b) Map of interpreted structural geometries in the 'tiger stripe' region from ~60°S to south pole allows c) a structural cross-section to be constructed and kinematics and dynamics to be reconstructed (modified from Yin and Pappalardo (2015)).

13.3. Reconstructing lost lithosphere using accretionary orogens

13.3.1 Building blocks of accretionary orogens

Once stable plate interiors and intra-plate deformation are reconstructed in a global plate circuit, all the gaps that remains in the global plate reconstruction represents lithosphere was lost to subduction. This area must largely have been occupied by oceanic lithosphere, but may also have contained microcontinents and arcs, as well as seamounts and oceanic plateaus (Figure 13.8). Those regions may have contained plate boundaries - mid-ocean ridges and transforms, even subduction zones - and entire plates may have disappeared. Reconstructing the nature and paleogeography of the plate boundaries and relative plate motions of this lost lithosphere is obviously more challenging than for major continents. It is even impossible if all lithosphere was subducted without accretion. But if accretion of rock units occurred at subduction zones, however little, first-order reconstructions of paleogeography and plates, and even lost-plate motions, may still be made, using geological records of accretionary orogens. In this section, we summarize the basic building blocks of accretionary orogens, how these may be used to reconstruct in tectonic and paleogeographic reconstruction, and how these inform about the composition of their slab remains that were recycled into the mantle.

During the process of subduction, rock units may decouple from the top of the downgoing plate and escape subduction. Such units may come in the form of thick packages of (deformed) stratigraphy and occasionally underlying crystalline basement - nappes - or as smaller blocks that mix with rock units of the hanging wall of the subducting plate - mélanges (e.g., Cawood *et al.* 2009)). Once decoupled from the subducting plate, they accrete to the upper plate - which is often undergoing intraplate deformation.

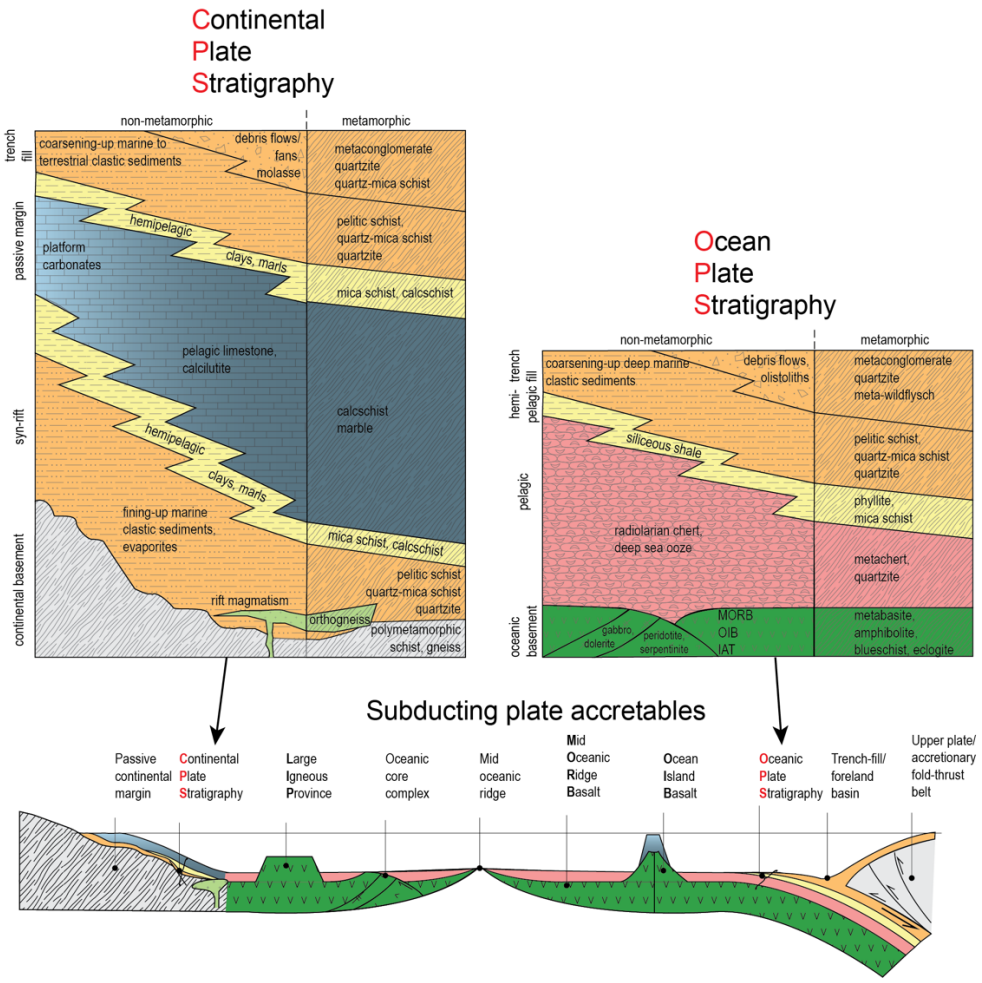

Figure 13.12: Top: typical stratigraphic sequences in non-metamorphic and metamorphic facies of continental crust-derived (CPS) and oceanic crust-derived (OPS) stratigraphic sequences that may be recognized in accreted nappes, or more chaotically, in mélanges Bottom: schematic representation of OPS and CPS in pre-subduction downgoing plate context. Modified after van Hinsbergen and Schouten (2021); Advokaat and van Hinsbergen (2024).

We may thus simplify orogens into 'upper/intraplate', and 'accretionary' parts (Fig. 13.8) (van Hinsbergen and Schouten 2021). As soon as rock units are accreted to the upper plate, they become entangled in intraplate deformation, and may thus experience multiphase deformation and associated metamorphism, leading to the complex geological records that orogens typically hold. But when the post-accretionary deformation and metamorphism, and associated (e.g., arc) magmatism is removed from their geological

history, the rock record of the accreted rock packages, whether nappes or mélanges, hold key clues that allow reconstructing the paleogeography and tectonic motions of the now-subducted plates that they originally were part of. There are essentially two types of accreted rock packages: ocean plate stratigraphy (OPS) and continental plate stratigraphy (CPS) (Fig. 13.12).

13.3.2 Ocean Plate Stratigraphy

Japanese geologist Yukio Isozaki and colleagues recognized in 1990 that the accreted nappes that make the accretionary orogen of Japan have a repeating, systematic stratigraphy. In their most complete form, these consist of pillow lavas at the base, followed by pelagic oceanic sediments (radiolarian cherts or red clays), and finally, thick, coarsening upward turbiditic sandstone-shale intercalations. They interpreted this sequence as the magmatic basement of an oceanic plate, followed by pelagic open-oceanic sediments and finally, trench fill clastics that were deposited shortly before the nappe underthrusted below and accreted to the upper plate (Figure 13.12). Isozaki *et al.* (1990) referred to this sequence as 'Ocean Plate Stratigraphy', or OPS, and explained how it holds critical information about the evolution of lost oceanic lithosphere. If the pillow lavas formed at a mid-ocean ridge (as may be inferred from a MORB geochemical signature), then the age difference between the lavas, or the oldest overlying pelagic sediments, and the foreland basin clastics provides a measure for the age of the oceanic plate during subduction. If the pillow lavas hold an ocean island basalt (OIB) or island arc tholeiite (IAT) composition, they represent the tops of accreted seamounts, and the age difference is only a minimum estimate for the age of the oceanic plate during subduction (see also Ueda (2006); Isozaki *et al.* (2010)) (Figure 13.12).

Accreted OPS sequences may escape metamorphism if they accreted at shallow crustal depth. However, when they decouple from the downgoing plate after significant burial, they undergo metamorphism. In mature subduction zones, metamorphism during rapid burial at plate tectonic rates leads to typical subduction zone metamorphism under

HP-LT conditions, transforming the mafic rocks into blueschists or eclogites. The timing of accretion of OPS sequences is bracketed between the youngest trench fill clastics and the oldest metamorphism. For overriding plates that are thinning through extension, such as in the Calabrian or Aegean regions during the Oligocene and Neogene (e.g., Brun and Faccenna (2008), the timing of climax pressure metamorphism coincides with the moment of accretion of the HP-LT metamorphic rocks from the downgoing to the overriding plate. However, when the upper plate is thickening through shortening, such as in Tibet, the increase of pressure may continue after accretion, and HP metamorphism only provides a minimum age for the timing of accretion van Hinsbergen *et al.* (2020a).

A special type of metamorphosed OPS is often found below ophiolites and is known as a metamorphic sole (Fig. 13.13). These are thin, typically a hundred to a few hundred meters thick, sheared and thrusted sequences of metabasalts and, in the deeper part, metasediments that are often found welded to the peridotite base of ophiolites (Jamieson 1986; Agard *et al.* 2016; Guilmette *et al.* 2018). Soles display an inverted metamorphic gradient: high-pressure, high-temperature garnet amphibolite or garnet granulite are found at the top of a sol, often only a few meters thick, which formed at ~8-15 kbar and 700-850°C (e.g., Jamieson 1986; Searle and Cox 2002; Guilmette *et al.* 2018). P and T conditions decrease downwards, where amphibolite and epidote amphibolite is found, also with mafic protolith, and greenschists that often also include metasedimentary rocks (Jamieson 1986; Kotowski *et al.* 2021).

Metamorphic soles are interpreted as remnants of oceanic crust (OPS) underthrust below mantle rock - and thus a former subduction interface. The portions of the sole with different P-T conditions coincide with separate thrust slices that accreted as the plate contact cools and decompresses (Soret *et al.* 2017; Kotowski *et al.* 2021; 2025). Sole zircon U/Pb crystallization ages and hornblende $^{40}Ar/^{39}Ar$ cooling ages almost always coincide with the age of crystallization of the crust of the supra-subduction zone ophiolites that currently overlies the sole (e.g., Hacker 1994; van Hinsbergen *et al.* 2015b; Rioux *et al.* 2016). Soles are therefore systematically the oldest and structurally highest 'nappes' of orogens and formed during the subduction initiation process.

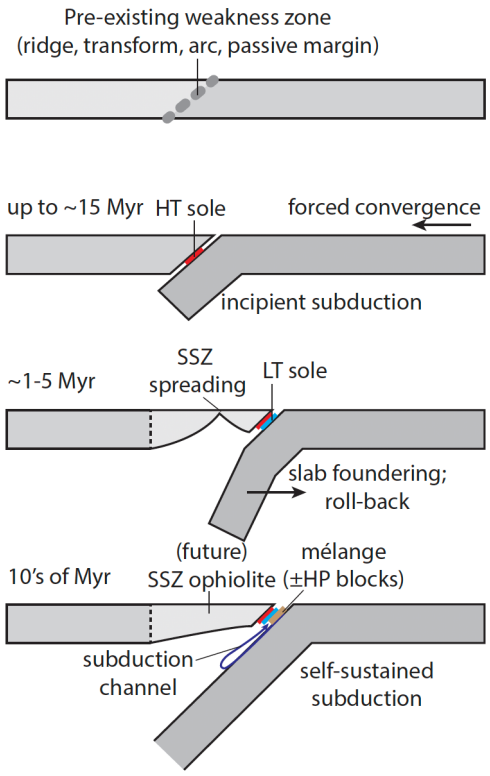

Figure 13.13: Cartoon cross-section of the conceptual evolution of a metamorphic sole, from Peters *et al.* (2026).

For a long time, the coincidence of zircon crystallization and cooling ages of metamorphic soles with SSZ ophiolite spreading was thought to show that the two formed simultaneously (e.g., Rioux *et al.* 2016), and the high temperatures were thus thought to show that subduction zones producing soles formed in a hot tectonic environment such as near a mid-oceanic ridge (Hacker 1991). However, recent Lu/Hf garnet geochronological data showed that sole growth precedes SSZ ophiolite spreading in the forearc of the incipient subduction zone (Guilmette *et al.* 2018; 2023; Mulcahy *et al.* 2018; Pourteau *et al.* 2019; Cunetta *et al.* 2025). And because soles are systematically associated with SSZ ophiolites that formed following subduction initiation at a variety of tectonic settings, metamorphic sole formation is not dependent on setting but are intrinsic to the subduction initiation process (Guilmette *et al.* 2023). SSZ ophiolites provides the mechanism through which soles are exhumed and become available for geological study, explaining the

systematic correlation (van Hinsbergen *et al.* 2015b). For reconstructions of orogenic belts, metamorphic soles are very useful: they signal the top of an accretionary orogen and the base of a (former) overriding plate, and date the onset of subduction.

The accretion of OPS is rare. The default behavior for oceanic lithosphere is subduction without accretion, or even with subduction erosion. For instance, there is no, or hardly any accretionary record of the 1000s of kms of oceanic lithosphere that subducted in Cenozoic time at the Andean, Tonga, Aleutian, Kuriles, or Marianas trenches. Besides Japan, well-known circum-Pacific OPS records of Mesozoic and Cenozoic age include those of New Zealand (Mortimer 2004), Costa Rica and Mexico (Kimbrough and Moore 2003; Buchs *et al.* 2013), and the Franciscan Complex of California (Wakabayashi 2015). Isozaki *et al.* (1990; 2010) pointed out that even within in the time windows during which these accretionary orogens formed, wholesale subduction was the default, and that brief episodes of accretion are intervened by long periods without accretion, or even with subduction erosion (von Huene *et al.* 2004), during which previously accreted records were dragged down into the subduction zone after all. Nonetheless, these highly incomplete accretionary records provide invaluable constraints on reconstructing the history and fate of lost oceanic plates.

Oceanic plates are in general large. The Pacific plate covers 20% of the Earth's surface and many of the smaller plates, such as Nazca or Juan de Fuca, are the remains of enormous plates if their subducted portions are considered. This means that even with little information, the motion history of such plates may be reconstructed at first order, working with simplest-case scenarios. For example, the age difference between the oldest pelagic sediments and the foreland basin clastics in the Hokkaido accretionary orogen of North Japan systematically decreased throughout the Mesozoic from at least 140 Myr in the late Jurassic and Early Cretaceous to only 20 Myr in the late Cretaceous, after which accreted lower Eocene trench fill clastics have intrusions of MORB basalt (Ueda 2006; Boschman *et al.* 2021a). This decrease in age of the subducted plate signals the approach of a mid-oceanic ridge towards the trench, whereby the early Eocene MORB intrusion into trench fill marks ridge subduction (Ueda 2006). This ridge must have been the plate

boundary between the Pacific plate and its conceptual northwestern conjugate Izanagi, and the timing of its subduction is consistent with e.g. changes in arc magmatism (Wu and Wu 2019).

Alternatively, stacked OPS nappes may contain sudden breaks in trends. For instance, a sudden change in ocean plate age inferred from the age difference between base and top of the chert sequence signals the subduction of a (former) plate boundary, such as a transform fault or a former intra-oceanic subduction zone. Out-of-sequence thrusting inferred from the ages of the trench fill of a consecutive series of nappes could signal the history of multiple subduction systems (Boschman *et al.* 2021a). Finally, collection of paleomagnetic data from such OPS sequences - from the pillow lavas or cherts - allows reconstructing the paleolatitudes of the ridges, or the seamounts built thereon, and provide another key constraint to develop quantitative plate kinematic reconstructions of lost oceanic lithosphere (e.g., Tarduno *et al.* (1985; 1986; Hagstrum and Sedlock 1992; Oda and Suzuki 2000; Boschman *et al.* 2021b). As sparse as OPS sequences may be compared to the vast areas of lost lithosphere that they were derived from, they provide a wealth of information on the restoration of the formation, motion, and demise of former oceanic plates.

13.3.3 Continental Plate Stratigraphy

A large volume of accreted rock units in orogenic belts is often derived from subducted continental margins or microcontinents. Majestic fold-thrust belts like the Himalaya, the Zagros, or the Mediterranean orogenic belts like the Apennines, Alps, Carpathians, or Aegean and Anatolian orogens, but also Taiwan, Timor, Cuba, and much of New Guinea, consist of nappes derived from continental lithosphere. Such nappes often account for a cumulative shortening of hundreds of, or even more than a thousand kilometers but contain only (upper) crustal portions stripped from their original lower crustal and mantle lithospheric underpinnings (e.g., van Hinsbergen *et al.* 2005; Capitanio *et al.* 2010; Handy *et al.* 2010). Although the stratigraphy of continental margins is more diverse than that of

oceanic crust, a first-order stratigraphic architecture may widely be recognized, which, in analogy to the OPS terminology of Isozaki *et al.* (2010), was named Continental Plate Stratigraphy (CPS) (van Hinsbergen and Schouten 2021).

CPS of accreted nappes consists in its simplest form of crystalline continental basement of an earlier orogenic phase overlain by syn-rift clastic sediments and associated rift-related magmatic rocks, post-rift passive margin sediments (van Hinsbergen and Schouten 2021) (Figure 13.12). And, finally, just like OPS, the highest stratigraphic unit of an accreted CPS is a sequence of foreland basin deposits. These deposits may be a deep marine turbidite sequence (a 'flysch'), such as deposited at present-day in the trough between Taiwan and mainland China, or a non-marine coarse clastic series ('molasse') such as in the Ganges floodplain of northern India in front of the Himalaya. Nonetheless, these mostly upper plate-derived continental clastics mark the arrival of CPS at a convergent plate boundary. The youngest foreland basin deposits of a CPS provide a maximum age, and the oldest ensuing metamorphism give a minimum age for the accretion of a CPS (Figure 13.12). The underlying passive margin units often consist of limestones, deep- or shallow marine, if paleoclimatic conditions were favorable. In colder environments, they may consist of fine-grained clastic pelagic sediments, or even diamictites marking the influence of ice cover (e.g., Eyles *et al.* 1983). These passive margin series may be thick, continuous sequences if paleo-water depth was deep enough or may contain hiatuses if depths were limited and eustatic sea level change could cause emergence. More complexly, continental margins may undergo multiple phases of extension (Reston 2005; Senkans *et al.* 2019; Gartrell *et al.* 2022) adding complexity and diversity to the CPS. Nonetheless, as a rule, each continental margin will at some stage in time have been formed by rifting of an originally larger continent which will be marked by the oldest syn-rift sequence. Such syn-rift sequences are typically fining-upward continental clastic series, often marine turbidite sequences, associated with mafic magmatic rocks related to decompression melting below the rift (Ziegler and Cloetingh 2004). Below the oldest syn-rift sediments eventually lies continental basement of an earlier orogenic phase. This may be Archean TTG basement, or remnants of an earlier accretionary orogen (e.g., Palin and

Santosh 2021), which consists of deformed and possibly metamorphosed OPS, CPS, or ophiolite and arc units (e.g., the Arabian-Nubian shield flanking the Red Sea (Stern 1994)).

If CPS underthrusts below the overriding plate prior to accretion, it may become metamorphosed. CPS nappes undergo HP-LT metamorphism when they are rapidly buried in subduction zones, as well-known from the Mediterranean region (Platt 1986; Jolivet *et al.* 2003; Brun and Faccenna 2008), the NW Himalaya (de Sigoyer *et al.* 2000), or the Greater Antilles in the Caribbean region (García-Casco *et al.* 2008). During their exhumation, either by return along the subduction interface, or in core complexes during upper plate extension (Jolivet *et al.* 2003), such metamorphosed CPS nappes tend to retain their internal stratigraphic and structural coherence (Brun and Faccenna 2008). Like for OPS units, accretion coincides with the timing of climax metamorphism if accretion occurs under an extensional and thinning upper plate but only provides a minimum estimate for accretion if the upper plates are thickening.

However, some accreted CPS units, for instance the Kırşehir and Menderes Massifs of Turkey, the deepest CPS nappe of the island of Naxos in Greece, were buried under much hotter conditions, and underwent 'Barrovian', HT-LP metamorphism (van Hinsbergen *et al.* (2025), see also Bird (1978) for an example from the Himalaya). Barrovian metamorphism is well-known from orogens but is normally inferred to result from the slow re-equilibration of the geotherm after orogenic crustal thickening, on timescales of tens of millions of years (England and Thompson 1984; Glazner and Bartley 1985). However, the examples above escaped HP-LT metamorphism and reached Barrovian conditions within only 5-10 Ma after they started to be underthrusted. A marked difference with HP-LT CPS units, which typically only comprise the passive margin sedimentary cover, these Barrovian CPS units are still underlain by their crystalline basement, in the Mediterranean region still 20-30 km. However, they are stripped from their pre-subduction lithospheric mantle, which subducted. Moreover, these Barrovian CPS nappes underthrusted far below the upper plate, in places even reaching the arc position, some ~150-200 km away from the trench. This may reflect the process of delamination of the downgoing continental lithosphere along the Moho during its subduction, or 'unzipping' (van Hinsbergen *et al.* 2025). The

mantle lithosphere subducts, but the buoyant crust is pushed below the base of the upper plate, where it becomes juxtaposed against the hot mantle wedge. This explains the high temperatures and avoids the drag-down into the subduction zone preventing the high-pressure conditions. The process may have been caught in the act in eastern Tibet, where unzipping of the east Indian continental margin below Tibet was recently inferred from seismological and geochemical data (Liu *et al.* 2025).

Whether CPS is dragged down deeply into a subduction zone to produce HP-LT metamorphism, or unzips and undergoes Barrovian metamorphism depends on the depth of decollement in the continental crust, which in turn may depend on crustal thickness. Stretched continental crust may subducts easier, leaving only the sedimentary cover behind, but when it becomes thicker, it may unzip instead. And when it is unstretched, it will resist subduction and eventually trigger slab break-off. Importantly, this depth of decollement may be a function of the geotherm, and unzipping may have been the more common response to continental subduction in a younger, hotter Earth.

13.3.4 Integrating multidisciplinary data

Reconstructions of tectonic history are much debated in the literature. Even for relatively straightforward tectonic puzzles such as the tectonic history and paleogeography in the Cretaceous and Cenozoic of the Indian and Asian plates preceding the onset of continental underthrusting that formed the Himalaya, the community has not found an agreement on the number of tectonic plates, continents, and subduction zones that were involved (Yin and Harrison 2000; Hu *et al.* 2016; Kapp and DeCelles 2019; Martin *et al.* 2020; van Hinsbergen 2022). For Paleozoic and older orogens, where plate circuit constraints are absent and geological records are less complete and often covered by basins and seas, reconstructions differ even more widely, even if there is a general agreement on the first-order architecture of the orogens on which the reconstruction is based. The most important source of this disagreement lies in the multidisciplinary nature of the observations that feed into such reconstructions.

A key problem in tectonics is the integration of the vast number of qualitative observations of the geological record into a coherent quantitatively described reconstruction. The chapters of this book nicely capture how widely varying the different sources of relevant information are. Sedimentology and stratigraphy, geo- and thermochronology, metamorphic geology, magmatic and isotope geochemistry, paleomagnetism, and structural geology all offer insights into relationships within the evolving solid earth that are relevant to the interpretation of tectonic problems. However, when taken out of their direct geological context, they provide the poor sod who is trying to make a reconstruction with a basket of apples and oranges.

Several problems arise when we try to integrate this diverse collection of data on the scale of a tectonic reconstruction. The relationships that are offered by the data types described in this book do not always provide strictly kinematic constraints but contain paleogeographic or dynamic interpretation. For instance, sediment provenance studies aim to link a clastic sedimentary deposit to its sink but need to invoke a distribution of land and sea. This requires mixing tectonic and paleogeographic reconstruction, and paleogeographic reconstruction, involving the interpretation of topography, bathymetry, and landforms, comes with its own set of difficulties. Geochemistry of magmatic rocks provides a valuable source of information but comes with a dynamic interpretation of geochemical cycling of e.g. elements that are brought down into a mantle wedge, produce partial melting, interact with upper plate crust, and find their way into a pluton or volcano. Tectonic reconstructions aim to provide a kinematic basis for dynamic interpretation and are thus best made with a minimum of dynamic interpretation.

The key problem is that by dividing the task of geological analysis over different communities, each with their own databases, we lose the original geological context - the field - from the analysis. The geological community is developing databases of geochronology, paleomagnetism, metamorphism, sedimentology, geochemistry, or structure that list data sets from a geographic region, whereby each dataset comes with an age uncertainty, and all those uncertainties are different. Tectonic reconstructions then try to integrate these databases again to display Earth's past in time slices, but we have no

systematic way to weight the effect of age uncertainty on reconstructions, and crosscutting relationships have been lost along the way. We tend to use the average age and have no systematic way of identifying which dataset is considered more informative than the next. This adds a level of subjectivity to the analysis that underlies the disparity in available reconstructions.

One way forward may be to integrate multidisciplinary data on a smaller scale of the building blocks of orogens, earlier in the tectonic analysis. A visual way to represent the different relevant datatypes are 'orogenic architecture diagrams' (Figure 13.14). There are various versions of such diagrams (e.g., Handy *et al.* 2010; van Staal *et al.* 2012; van Hinsbergen *et al.* 2020b; Wakabayashi 2021; Advokaat and van Hinsbergen 2024). The version in Figure 13.14 is by Maremmani *et al.* (2025) who developed a template to display the geological history of nappes and its structural relations with adjacent nappes. When viewed on the scale of for instance one nappe of OPS or CPS, the integration of data is easier and more conclusive. Nappes contain a stratigraphic coherence that - independent of how well we can numerically date the rocks - show what came first and last. Clastic sedimentary rocks in this stratigraphy may then be used to infer changes in sediment provenance throughout the history of this concentrated package of rock. Within the same stratigraphy, paleomagnetic data may demonstrate paleolatitudinal change and vertical axis rotation, geochemical data of magmatism offer insight into processes along the way. Structural data demonstrate deformation during sedimentation and thereafter and give a next series of relative timing through cross-cutting relationships and combined with metamorphic data and perhaps igneous intrusions reveal the history of a nappe after incorporation into orogens. Tectonic reconstructions (in terms of processes like continental break-up, subduction, suturing, collision, obduction) then need to integrate the interpretations of integrated histories of the orogen's building blocks (in terms of subsidence, sedimentation, paleolatitudinal drift, burial, deformation, recrystallization, intrusion). This way, the sources of conflicting interpretations may be directly linked to the field context, and tectonic reconstructions may be better interrogated by targeted field and laboratory research.

The building blocks may then be integrated in quantitative tectonic reconstructions of global plate motion (e.g., van Hinsbergen and Schmid 2012), for examples of methodology to restore the Aegean nappes in the Cenozoic). The diagrams summarize when nappes transferred from a downgoing to an overriding plate - e.g., bracketed by the time interval between the youngest trench fill deposits and the oldest metamorphism. Reconstructions of intraplate deformation restore the deformation that the nappes underwent after accretion. They are then, at the moment of accretion, re-connected to the downgoing plate, and 'unsubducted' back in time (e.g., the Pacific Plate highlighted in Fig. 13.3). With constraints from paleomagnetism, paleontology, and/or sediment provenance, they may then be restored farther back in time (Boschman *et al.* 2021b). This procedure then leads to a relative plate motion reconstruction of rigid plates, deformed plates, and subducted plates.

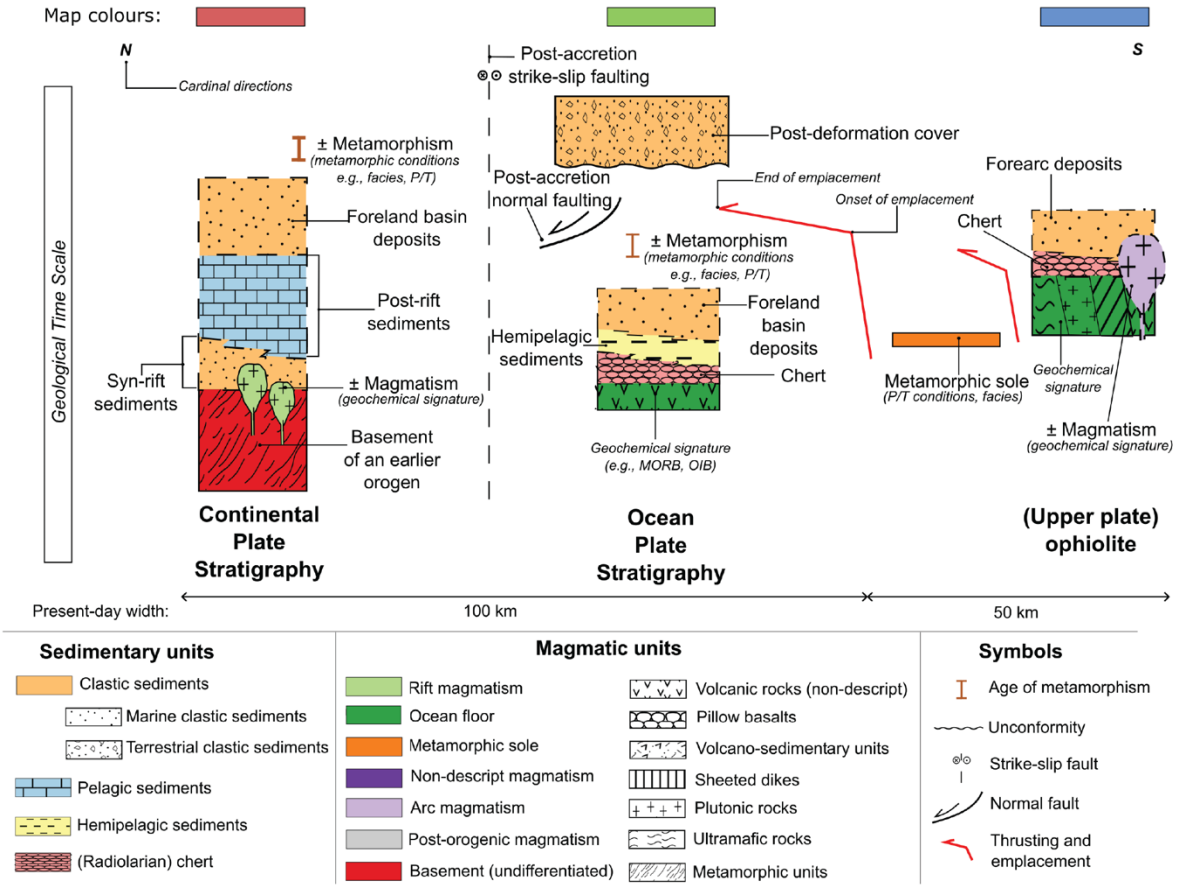

Figure 13.14: Summary of how geological constraints relevant for tectonic reconstruction may be integrated per accreted OPS, CPS, or Ophiolite unit in orogenic architecture diagrams (from Maremmani *et al.* 2025).

13.4 Reference frames

Relative plate reconstructions as outlined in the previous sections are sufficient to interpret any geological process that requires knowledge of relative motion. For instance, if one aims to interpret how much orogenic shortening occurred during the convergence of two plates, either one of those plates can be taken as fixed and the answer remains the same. However, for paleoclimatology or paleobiology problems, or for geodynamic analysis that integrates the plate motion and tectonic deformation with motions in the dynamic mantle, a relative plate reconstruction needs to be placed in the relevant reference frame (Figure 13.15). Changing a reference frame to a reconstruction is simple: relative plate motion reconstructions are all made relative to one 'root' plate - in the case of default GPlates reconstructions, (South) Africa. All that is required is a set of Euler rotations that places South Africa relative to the chosen reference (e.g., Tables 13.1 and 13.2), and the rest of the reconstruction will follow.

Paleoclimate and paleobiology problems are based on e.g. fossil and isotope records, and to interpret these correctly, it is important to determine their paleolatitudinal context that controls the angle of insolation, the prime control on regional climate. For all problems related to paleoclimate and environment, it is therefore important to place plate reconstructions relative to the Earth's spin axis. There are two processes that controlled how rock units, or fossils therein, moved relative to the Earth's spin axis after their formation: plate motion relative to the mantle, and 'true polar wander': the rotation of the mantle and plates together relative to the Earth's spin axis (Goldreich and Toomre 1969). True Polar Wander is the result of changes in Earth's moment of inertia that result from processes that change its density structure, notably sinking slabs, rising plumes, and dynamic topography (Steinberger and Torsvik 2010). True Polar Wander occurs at rates that are similar as plate motions and may culminate amount of thousands of kilometers of

paleolatitudinal change (Torsvik *et al.* 2014; Vaes and van Hinsbergen 2025), and is thus important to take into account when interpreting paleogeography, -climate, and -biology. To this end, the plate reconstruction must be placed in a paleomagnetic reference frame (e.g., van Hinsbergen *et al.* 2015a) that may be computed from a global apparent polar wander path (e.g., Besse and Courtillot 2002; Torsvik *et al.* 2012; Vaes *et al.* 2023); see Chapter 12 by (Fu and van Hinsbergen 2026)) (Fig. 13.15). For example, Table 13.1 shows the Euler rotations that places South Africa relative to the Earth's spin axis using the most global apparent polar wander path of Vaes *et al.* (2023). Finally, to interpret paleoclimate, the motions of the spin axis relative to Earth's orbit (Milankovitch' precession and obliquity cycles) and in the shape of Earth's orbit (eccentricity) need to be considered, but that is beyond the scope of (plate) tectonic reconstruction.

Geodynamic studies aim to decipher the relationships between the tectonic plates and their deformation and magmatism, and the underlying convecting mantle. Therefore, a reference frame must be chosen that estimates how plates moved over the mantle, and in which the effects of TPW are not visible, through a 'mantle reference frame'. Such mantle reference frames are often based on correlations between elements in the non-lithospheric mantle and the surface plates that appear to yield reasonable approximations of plate-mantle motion: tracks of hotspot volcanoes and their asthenospheric melt sources interpreted as deep-mantle plumes (e.g., Müller *et al.* 1993; Torsvik *et al.* 2019; Gaastra *et al.* 2022) (Fig. 13.15), mantle plume-related magmatism and possible plume source regions in the lowermost mantle (Torsvik *et al.* 2010; 2014), or subducted slabs and subduction-related orogens and arcs (van der Meer *et al.* 2010). However, it is important to realize that mantle reference frames are paradoxical, because by defining the mantle as a reference requires assuming that it may be treated a fixed object. If the mantle is convecting, there is no such thing as a 'mantle reference frame'. For instance, hotspot sources have been shown to move relative to each other at rates of mm/yr (Steinberger 2000). Such motions may thus be used to constrain mantle convective behavior - so-called 'moving hotspot frames' are numerical models of mantle convection that are iteratively tuned against hotspot motions (e.g., O'Neill *et al.* 2005; Torsvik *et al.* 2008; Doubrovine *et*

al. 2012). However, these are not kinematic 'reference frames', but dynamic models that depend on a wide range of assumptions of the mantle properties that we aim to study using kinematic observations.

Table 13.1: Example of a paleomagnetic reference frame in GPlates rotation format. This table lists total reconstruction poles that rotate South Africa (701) from its present-day location into its position relative to the geomagnetic pole, assumed to align with the spin axis (1) for selected times, using the site-level global apparent polar wander of Vaes *et al.* (2023)

Reconstructed plate ID	age	lat	lon	rotation	reference plate ID
701	0.0	0.0	0.0	0.0	1
701	1.3	0.0	43.2	0.4	1
701	4.4	0.0	64.1	2.1	1
701	21.7	0.0	99.4	7.3	1
701	28.2	0.0	113.2	9.2	1
701	37.5	0.0	116.1	10.4	1
701	56.1	0.0	121.0	14.8	1
701	60.0	0.0	125.2	16.3	1
701	64.7	0.0	129.1	16.9	1
701	82.0	0.0	141.5	17.4	1
701	89.7	0.0	154.9	21.8	1
701	94.6	0.0	161.5	25.8	1
701	114.7	0.0	170.7	32.1	1
701	120.2	0.0	170.0	35.0	1
701	131.0	0.0	172.7	39.3	1
701	134.2	0.0	174.1	40.0	1
701	152.4	0.0	173.7	36.6	1
701	158.7	0.0	173.1	34.2	1
701	172.6	0.0	168.6	31.1	1
701	182.1	0.0	169.5	25.8	1
701	189.7	0.0	165.3	24.2	1
701	203.7	0.0	153.5	24.6	1
701	209.7	0.0	148.1	27.1	1
701	217.5	0.0	143.8	30.5	1
701	224.4	0.0	143.1	33.3	1

701	242.5	0.0	148.3	43.2	1
701	253.3	0.0	151.7	47.3	1
701	257.2	0.0	152.4	47.9	1
701	268.6	0.0	148.5	49.0	1
701	281.3	0.0	146.2	53.1	1
701	288.4	0.0	147.0	55.4	1
701	397.8	0.0	142.1	59.2	1
701	311.1	0.0	135.3	63.4	1
701	320.3	0.0	129.8	61.8	1

Table 13.2: Example of a mantle reference frame in GPlates rotation format. This table lists total reconstruction poles, which rotate South Africa (701) from its present-day location into its position relative to a hypothetical stagnant mantle (0) for selected times, using the minimum-continent-motion reference frame of Wagenaar *et al.* (2025).

Reconstructed plate ID	age	lat	lon	rotation	reference plate ID
701	10	20.1	-26.7	-1.2	0
701	20	19.2	-23.1	-2.4	0
701	30	26.9	-21.4	-4.5	0
701	40	-29.6	158.5	7.1	0
701	50	-31.8	157.4	9.4	0
701	60	-32.6	154.4	10.7	0
701	70	-33.1	155.0	12.1	0
701	80	-34.4	156.9	15.7	0
701	90	35.3	-20.9	-20.2	0
701	100	35.4	-20.8	-25.6	0
701	110	34.9	-19.7	-31.2	0
701	120	33.5	-18.0	-37.1	0
701	130	32.4	-16.9	-39.6	0
701	140	31.2	-16.8	-41.3	0
701	150	30.7	-17.0	-42.2	0
701	160	29.7	-16.5	-43.3	0
701	170	28.8	-15.6	-44.7	0
701	180	28.5	-14.8	-45.3	0
701	190	28.4	-14.1	-45.7	0
701	200	28.3	-13.4	-46.0	0
701	350	28.3	-13.4	-46.0	0

	Mantle reference	Paleomagnetic reference
Definition	• coordinate system that attempts to estimate motion of plates relative to the mantle	• coordinate system that considers the motion of tectonic plates relative to Earth's spin axis
Application	• plate tectonic studies • geodynamics • slab reconstructions	• paleomagnetic studies • paleoclimate, paleobiology, paleoceanography

Examples

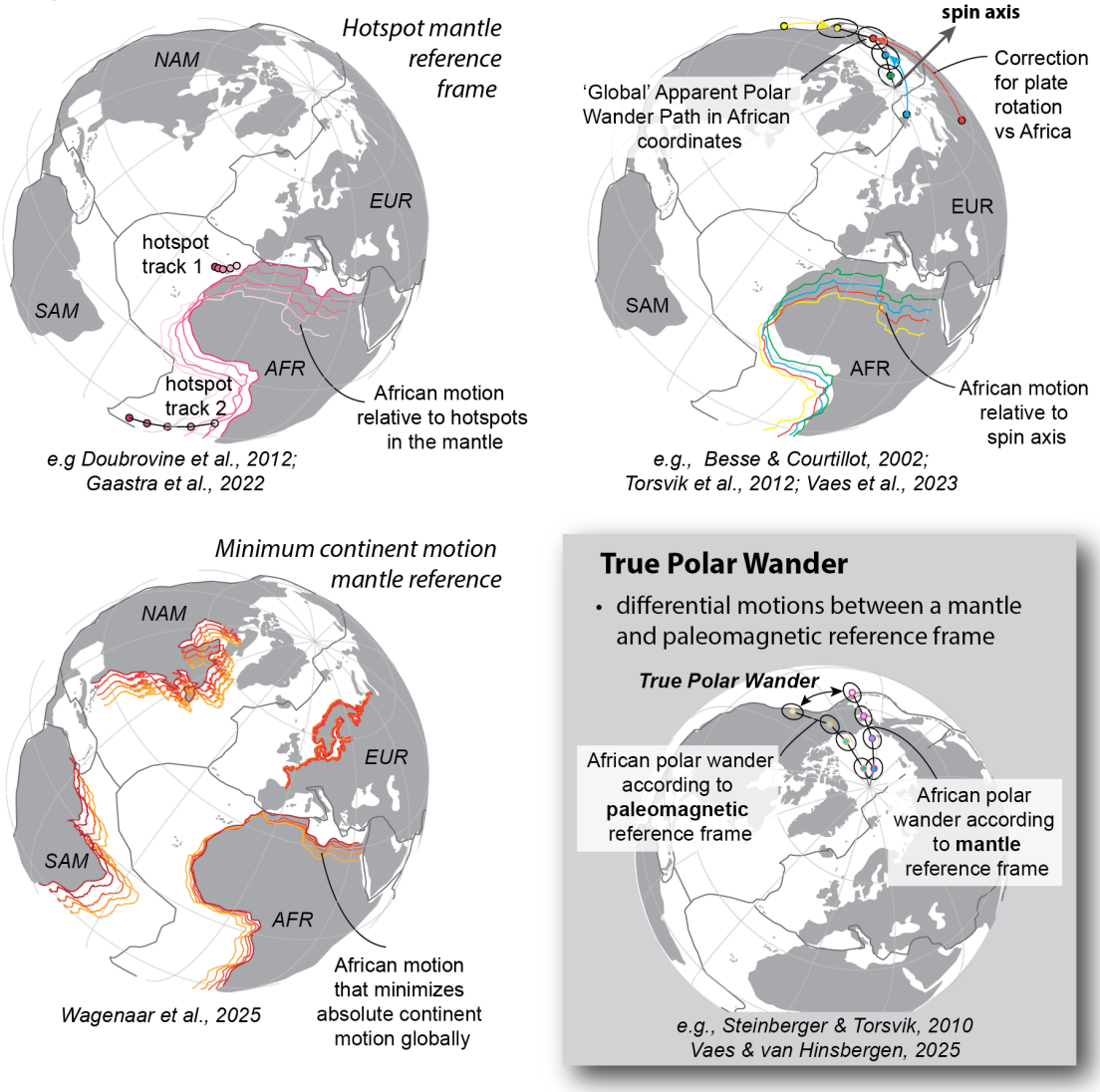

Figure 13.15. Summary of the basic principles of paleomagnetic and mantle reference frames, and the difference between them caused by true polar wander.

Differences between mantle reference frames are interesting and require an explanation. Assuming that they may be the result of uncertainties within each approximation of the mantle reference frame, Tetley *et al.* (2019) and Müller *et al.* (2022) developed a 'tectonic rules' frame, whereby several different approaches (hotspot tracks, minimizing continent and trench motions, and limiting net lithosphere rotation) were combined, and assigned equal weight. The benefit of such a tectonic rules approximation is that it can be computed for the whole duration of a plate reconstruction, whereas frames using hotspots are restricted to the last 100-150 Ma (Müller *et al.* 1993; Torsvik *et al.* 2019). However, they come without quantified uncertainty, as it is not possible to determine how each rule should be weighted. To overcome this, Wagenaar *et al.* (2025) recently developed a mantle reference frame based on only one of these rules: Assuming that the non-lithospheric mantle is stagnant, the Euler rotation of Africa in 10 Myr time steps that involves the smallest motion of global continental area, represents absolute plate motion (Fig. 13.15). As a proxy for uncertainty, Wagenaar *et al.* (2025) evaluated the effects of a 5 Myr uncertainty in the age of the plate reconstruction (e.g., the reconstruction at 50 Ma may be represented by any configuration in the 45 to 55 Ma time interval), they showed that the minimum-continent-motion frame resolves absolute plate motion for the last 350 Ma. For times prior, the uncertainty of the steps exceeds the steps themselves, and absolute plate motion is unresolved.

13.5 New frontiers in reconstructions: mantle tectonics

Finally, the new frontier in tectonic reconstruction is taking up the challenge to reconstruct mantle convection. A rapidly developing frontier in solid earth science is the mapping of the structure of the mantle from seismology (see Kufner et al., Chapter 5), and the geological interpretation of its history that may be tied to geological observations in the relative plate model. This paves the way to tectonically reconstruct the yet unknown convective motions in the mantle. We here summarize reconstruction approaches that are being developed based on seismic tomographic imaging of the mantle. This section is not

comprehensive: there are more avenues into exploring mantle structure, composition, and history. This includes other seismological techniques, such as seismic anisotropy (e.g., Wolf and Long(2023) or attenuation Talavera-Soza *et al.* (2025). Geochemistry of magmatic rocks (Richter *et al.* 2020; Urann *et al.* 2020; Liu *et al.* 2022; Stracke *et al.* 2022) reveals the compositional of the mantle that results from its geological history. A growing third avenue is geochronology of zircon xenocrysts that come up in oceanic intraplate volcanoes or at mid-oceanic ridges, which reveal the remnants of ancient mantle plumes or subduction-related mantle wedges (Pilot *et al.* 1998; Cheng *et al.* 2016; Bea *et al.* 2020; Greenough *et al.* 2021; Rojas-Agramonte *et al.* 2022; 2024). Integrating such geochemical and geochronological datasets with plate reconstructions and seismology may offer novel ways to decipher motions in the mantle in the future. The examples below of mantle reconstruction focus on the use of remnants of subducted slabs.

Seismological research has identified wave speed anomalies in the mantle that form predominantly due to some combination of temperature. Low wave-speed anomalies, although challenging to resolve, supported (Morgan 1971)'s hypothesis that long-lived hotspots are fed by mantle plumes that originate in the deep mantle (e.g., Boschi *et al.* 2007; Nolet *et al.* 2007; Zhao 2007). Moreover, they revealed spatial correlation of such plumes to the edges of two enigmatic, large low shear-wave velocity provinces (LLSVPs) (Garnero 2000; McNamara 2019), whose geological history remains poorly understood but that appear to be long-lived phenomena that existed throughout the Phanerozoic (Torsvik *et al.* 2010).

High-wavespeed anomalies, on the other hand, have since the early days of seismic tomography, systematically ben found dipping into the mantle at modern subduction zones and became interpreted as slabs of subducted lithosphere (Spakman *et al.* 1988; van der Hist *et al.* 1991). With the advent of whole-mantle tomography, it became clear that such high wavespeed anomalies cross the upper-lower mantle boundary (Grand *et al.* 1997; Bijwaard *et al.* 1998), where they form thickened continuations of upper mantle slabs. Examples are the African slab below the Aegean region (Faccenna *et al.* 2003; van Hinsbergen *et al.* 2005), the Pacific slab below the Mariana arc (Miller *et al.* 2005), or the

major Farallon slab subducting below Mexico (Grand *et al.* 1997; Boschman *et al.* 2018). This showed that subducted slabs enter the lower mantle and can still be resolved, and that lower mantle anomalies that are no longer connected to the surface may also represent subducted lithosphere (e.g., Van der Voo *et al.* 1999a, b; Hafkenscheid *et al.* 2006).

Following these developments, van der Meer *et al.* (2010; 2018) made a systematic geological interpretation of high wavespeed tomographic anomalies, correlating shallower slabs to younger orogens and deeper slabs to older orogens, assuming that slabs do not change position relative to each other after they broke off from the plate circuit. This revealed that (i) all upper mantle slabs are explained by Cenozoic subduction; (ii) lower mantle slabs are thickened and sink much slower than upper mantle slabs (~0.5-1.5 cm/a, varying with depth (van der Meer *et al.* 2018); (iii) the modern configuration of slabs still mimics the pattern of subduction zones at which they subducted suggesting near-vertical sinking after break-off (van der Meer *et al.* 2014; Domeier *et al.* 2016); (iv) there are no geologically documented records of Mesozoic and Cenozoic subduction that cannot be correlated to upper or lower mantle anomalies, so slabs do not appear to entirely thermally assimilate into the mantle before they reach the core-mantle boundary; and (v) slabs are still able to reach the core-mantle boundary despite billions of years of subduction, so the remains of older slabs must have been advected back into the mantle. Finally, there are more high-wavespeed anomalies than can be explained by subduction (e.g., Schouten *et al.* 2024), which may represent delaminated lithosphere, regions with higher water content, or other, still unknown causes.

These 1D correlations offered insight in the rate of the vertical component of mantle convection. Slab sinking rates in the lower mantle of 1.5 cm/yr or less are much slower than plate motion rates. Hence, ambient mantle convection rates must be even slower (e.g., Čížková *et al.* 2012; van der Wiel *et al.* 2024a). Moreover, given that globally averaged subduction rates are ~6 cm/yr (Schellart 2008; van der Meer *et al.* 2014), slabs must on average thicken by a factor of 4 or more on their way down into the lower mantle.

Numerical modeling suggested that the slabs may thicken by buckling in the mantle transition zone (Ribe and al. 2007; Goes *et al.* 2017). Wu *et al.* (2016) therefore studied the shapes of slabs in the transition zone and below in detail, and for a case study in SE Asia, successfully unfolded these slabs, restoring the original area they once occupied prior to subduction (Fig. 13.16). They showed that the slabs in the upper ~1000 km of the mantle indeed represented the area lost to subduction since the late Cretaceous. Subsequent analyses of the slabs below South America (Chen *et al.* 2019), Alaska (Fuston and Wu 2021) and the eastern Caribbean region (Chen *et al.* 2024) further showed how quantitative reconstructions of area loss due to subduction may be reconstructed from seismic images of the mantle and may be reconciled with plate kinematic reconstructions.

Van der Meer *et al.* (2012) took it a step further, by using seismic tomographic images as constraint on plate tectonic reconstructions. They inferred that a large, N-S trending band of slabs in the lower mantle below the modern Pacific Ocean represents a former intra-oceanic subduction zone in the Mesozoic Panthalassa Ocean - a hypothesis later shown to be consistent with independent plate kinematic constraints based on restoration of the circum-Philippine Sea Plate accretionary orogens (van de Lagemaat *et al.* 2024; van de Lagemaat and van Hinsbergen 2024). Sigloch and Mihalynuk (2013; 2017), and later Clennett *et al.* (2020) developed this further in a 'tomo-tectonic' analysis of the eastern Panthalassa domain, using seismic tomographic images to infer the location and age of subduction systems that led to the Cordilleran orogeny along the western North American margin. It should be noted, however, that such analyses use average slab sinking rates to determine which slab belongs to which orogenic record, and require assuming that modern slab locations are representative for the location of subduction, i.e., that slabs sink vertically. The tomo-tectonic approach thus requires assuming knowledge about mantle motion to inform plate tectonic evolution, and do not provide constraints on the kinematic evolution of the mantle.

The two decades of analyses of mantle-geology correlations have slowly demonstrated how the mantle may be tectonically reconstructed. Nonetheless, mantle tectonics is still in its infancy, and great challenges to unify the different eyes into mantle structure and

composition remain. Nonetheless, tectonic reconstruction of the mantle is key to decipher the dynamics that govern solid earth evolution and is an avenue worth pursuing in the future - in a similar integrative, multidisciplinary way as plate tectonics and orogenic reconstruction has been in the last 60 years.

13.6 References

Advokaat, E.L. and van Hinsbergen, D.J.J. 2024. Finding Argoland: reconstructing a microcontinental archipelago from the SE Asian accretionary orogen. *Gondwana Research*, **128**, 161-263.

Agard, P., Yamato, P., Soret, M., Prigent, C., Guillot, S., Plunder, A., Dubacq, B., Chauvet, A. and Monié, P. 2016. Plate interface rheological switches during subduction infancy: Control on slab penetration and metamorphic sole formation. *Earth and Planetary Science Letters*, **451**, 208-220.

Allerton, S. and Vine, F. 1987. Spreading structure of the Troodos ophiolite, Cyprus: Some paleomagnetic constraints. *Geology*, **15**, 593-597.

Anonymous 1972. Penrose field conference on ophiolites. *Geotimes*, **17**, 24-25.

Arkula, C., Lom, N., Wakabayashi, J., Rea-Downing, G., Qayyum, A., Dekkers, M.J., Lippert, P.C. and van Hinsbergen, D.J.J. 2023. The forearc ophiolites of California formed during trench-parallel spreading: Kinematic reconstruction of the western USA Cordillera since the Jurassic. *Earth-Science Reviews*, **237**, 104275.

Avouac, J.P., Tapponnier, P., Bai, M., You, H. and Wang, G. 1993. Active thrusting and folding along the northern Tien Shan and late Cenozoic rotation of the Tarim relative to Dzungaria and Kazakhstan. *Journal of Geophysical Research: Solid Earth*, **98**, 6755-6804.

Bandyopadhyay, D., van Hinsbergen, D.J.J., Plunder, A., Bandopadhyay, P.C., Advokaat, E., Chattopadhaya, S., Morishita, T. and Ghosh, B. 2020. Andaman Ophiolite: An Overview. *In*: Ray, J.S. and Radhakrishna, M. (eds) *The Andaman Islands and Adjoining Offshore: Geology, Tectonics and Palaeoclimate*. Springer International Publishing, Cham, 1-17, https://doi.org/10.1007/978-3-030-39843-9_1.

Bea, F., Bortnikov, N., Montero, P., Zinger, T., Sharkov, E., Silantiev, S., Skolotniev, S., Trukhalev, A. and Molina-Palma, J.F. 2020. Zircon xenocryst evidence for crustal recycling at the Mid-Atlantic Ridge. *Lithos*, 105361.

Besse, J. and Courtillot, V. 2002. Apparent and true polar wander and the geometry of the geomagnetic field over the last 200 Myr. *Journal of Geophysical Research: Solid Earth*, **107**, EPM 6-1-EPM 6-31, https://doi.org/10.1029/2000jb000050.

Bijwaard, H., Spakman, W. and Engdahl, E.R. 1998. Closing the gap between regional and global travel time tomography. *Journal of Geophysical Research: Solid Earth*, **103**, 30055-30078, https://doi.org/10.1029/98jb02467.

Bird, P. 1978. Initiation of intracontinental subduction in the Himalaya. *Journal of Geophysical Research: Solid Earth*, **83**, 4975-4987.

Bird, P. 2003. An updated digital model of plate boundaries. *Geochemistry, Geophysics, Geosystems*, **4**.
Bortolotti, V., Chiari, M., Marroni, M., Pandolfi, L., Principi, G. and Saccani, E. 2013. Geodynamic evolution of ophiolites from Albania and Greece (Dinaric-Hellenic belt): one, two, or more oceanic basins? *International Journal of Earth Sciences*, **102**, 783-811, https://doi.org/10.1007/s00531-012-0835-7.
Boschi, L., Becker, T. and Steinberger, B. 2007. Mantle plumes: Dynamic models and seismic images. *Geochemistry, Geophysics, Geosystems*, **8**.
Boschman, L.M., van Hinsbergen, D.J.J. and Spakman, W. 2021a. Reconstructing Jurassic-Cretaceous intra-oceanic subduction evolution in the northwestern Panthalassa Ocean using Ocean Plate Stratigraphy from Hokkaido, Japan. *Tectonics*, **40**, e2019TC005673.
Boschman, L.M., van Hinsbergen, D.J.J., Torsvik, T.H., Spakman, W. and Pindell, J.L. 2014. Kinematic reconstruction of the Caribbean region since the Early Jurassic. *Earth-Science Reviews*, **138**, 102-136, https://doi.org/10.1016/j.earscirev.2014.08.007.
Boschman, L.M., van Hinsbergen, D.J.J., Kimbrough, D.L., Langereis, C.G. and Spakman, W. 2018. The dynamic history of 220 million years of subduction below Mexico: a correlation between slab geometry and overriding plate deformation based on geology, paleomagnetism, and seismic tomography. *Geochemistry, Geophysics, Geosystems*, **19**, 4649-4672.
Boschman, L.M., Van Hinsbergen, D.J.J., Langereis, C.G., Flores, K.E., Kamp, P.J.J., Kimbrough, D.L., Ueda, H., van de Lagemaat, S.H.A., Van der Wiel, E. and Spakman, W. 2021b. Reconstructing lost plates of the Panthalassa Ocean through paleomagnetic data from circum-Pacific accretionary orogens. *American Journal of Science*, **321**, 907-954.
Brun, J.-P. and Faccenna, C. 2008. Exhumation of high-pressure rocks driven by slab rollback. *Earth and Planetary Science Letters*, **272**, 1-7, https://doi.org/10.1016/j.epsl.2008.02.038.
Buchs, D.M., Pilet, S., Cosca, M., Flores, K.E., Bandini, A.N. and Baumgartner, P.O. 2013. Low-volume intraplate volcanism in the Early/Middle Jurassic Pacific basin documented by accreted sequences in Costa Rica. *Geochemistry, Geophysics, Geosystems*, **14**, 1552-1568, https://doi.org/10.1002/ggge.20084.
Buffan, L., Jones, L.A., Domeier, M., Scotese, C.R., Zahirovic, S. and Varela, S. 2023. Mind the uncertainty: Global plate model choice impacts deep-time palaeobiological studies. *Methods in Ecology and Evolution*, **14**, 3007-3019.
Capitanio, F.A., Morra, G., Goes, S., Weinberg, R.F. and Moresi, L. 2010. India–Asia convergence driven by the subduction of the Greater Indian continent. *Nature Geoscience*, **3**, 136-139, https://doi.org/10.1038/ngeo725.
Cascioli, G., Gülcher, A.J., Mazarico, E. and Smrekar, S.E. 2025. A spectrum of tectonic processes at coronae on Venus revealed by gravity and topography. *Science Advances*, **11**, eadt5932.
Casey, J.F. and Dewey, J.F. 1984. Initiation of subduction zones along transform and accreting plate boundaries, triple-junction evolution, and forearc spreading centres—

implications for ophiolitic geology and obduction. *Geological Society, London, Special Publications*, **13**, 269-290, https://doi.org/10.1144/gsl.Sp.1984.013.01.22.
Cawood, P., Pisarevsky, S.A. and Leitch, E. 2011. Unraveling the New England orocline, east Gondwana accretionary margin. *Tectonics*, **30**.
Cawood, P.A., Kröner, A., Collins, W.J., Kusky, T.M., Mooney, W.D. and Windley, B.F. 2009. Accretionary orogens through Earth history. *Geological Society, London, Special Publications*, **318**, 1-36.
Chen, Y.-W., Wu, J. and Suppe, J. 2019. Southward propagation of Nazca subduction along the Andes. *Nature*, **565**, 441.
Chen, Y.-W., Wu, J. and Goes, S. 2024. Lesser Antilles slab reconstruction reveals lateral slab transport under the Caribbean since 50 Ma. *Earth and Planetary Science Letters*, **627**, 118561.
Cheng, H., Zhou, H., Yang, Q., Zhang, L., Ji, F. and Dick, H. 2016. Jurassic zircons from the Southwest Indian Ridge. *Scientific Reports*, **6**, 26260.
Čížková, H., van den Berg, A.P., Spakman, W. and Matyska, C. 2012. The viscosity of Earth's lower mantle inferred from sinking speed of subducted lithosphere. *Physics of the Earth and Planetary Interiors*, **200-201**, 56-62, https://doi.org/10.1016/j.pepi.2012.02.010.
Clennett, E.J., Sigloch, K., Mihalynuk, M.G., Seton, M., Henderson, M.A., Hosseini, K., Mohammadzaheri, A., Johnston, S.T. and Müller, R.D. 2020. A quantitative tomotectonic plate reconstruction of western North America and the eastern Pacific basin. *Geochemistry, Geophysics, Geosystems*, **21**, e2020GC009117.
Collins, G.C., Patterson, G.W., Detelich, C.E., Prockter, L.M., Kattenhorn, S.A., Cooper, C.M., Rhoden, A.R., Cutler, B.B., Oldrid, S.R. and Perkins, R.P. 2022. Episodic Plate tectonics on Europa: Evidence for widespread patches of mobile-lid behavior in the antijovian hemisphere. *Journal of Geophysical Research: Planets*, **127**, e2022JE007492.
Cowgill, E., Yin, A., Harrison, T.M. and Wang, X.-F. 2003. Reconstruction of the Altyn Tagh fault based on U-Pb geochronology: Role of back thrusts, mantle sutures, and heterogeneous crustal strength in forming the Tibetan Plateau. *Journal of Geophysical Research: Solid Earth*, **108**, https://doi.org/10.1029/2002jb002080.
Cox, A. and Hart, R.B. 1986. *Plate tectonics: how it works*. John Wiley & Sons.
Cunetta, N.S., Mulcahy, S.R., Schermer, E.R. and Smit, M.A. 2025. Early Jurassic subduction initiation recorded in the Easton metamorphic suite, Northwest Cascades (Washington, USA). *Geological Society of America Bulletin*, **137**, https://doi.org/https://doi.org/10.1130/B38167.1.
Cunningham, D. 2005. Active intracontinental transpressional mountain building in the Mongolian Altai: Defining a new class of orogen. *Earth and Planetary Science Letters*, **240**, 436-444, https://doi.org/10.1016/j.epsl.2005.09.013.
Cunningham, W. and Mann, P. 2007. Tectonics of strike-slip restraining and releasing bends. *Geological Society, London, Special Publications*, **290**, 1-12.
de Sigoyer, J., Chavagnac, V., Blichert-Toft, J., Villa, I.M., Luais, B., Guillot, S., Cosca, M. and Mascle, G. 2000. Dating the Indian continental subduction and collisional thickening in the northwest Himalaya: Multichronology of the Tso Morari eclogites. *Geology*, **28**, 487-490.

DeCelles, P.G. and Horton, B.K. 2003. Early to middle Tertiary foreland basin development and the history of Andean crustal shortening in Bolivia. *Geological Society of America Bulletin*, **115**, 58-77.
DeMets, C. and Merkouriev, S. 2021. Detailed reconstructions of India–Somalia Plate motion, 60 Ma to present: implications for Somalia Plate absolute motion and India–Eurasia Plate motion. *Geophysical Journal International*, **227**, 1730-1767.
Dewey, J. and Casey, J. 2011. The origin of obducted large-slab ophiolite complexes *Arc-Continent Collision*. Springer, 431-444.
Dewey, J.F. 1976. Ophiolite obduction. *Tectonophysics*, **31**, 93-120.
Domeier, M. and Torsvik, T.H. 2014. Plate tectonics in the late Paleozoic. *Geoscience Frontiers*, **5**, 303-350, https://doi.org/10.1016/j.gsf.2014.01.002.
Domeier, M., Doubrovine, P.V., Torsvik, T.H., Spakman, W. and Bull, A.L. 2016. Global correlation of lower mantle structure and past subduction. *Geophysical Research Letters*, **43**, 4945-4953, https://doi.org/10.1002/2016gl068827.
Doubrovine, P.V. and Tarduno, J.A. 2008. Linking the Late Cretaceous to Paleogene Pacific plate and the Atlantic bordering continents using plate circuits and paleomagnetic data. *Journal of Geophysical Research*, **113**, https://doi.org/10.1029/2008jb005584.
Doubrovine, P.V., Steinberger, B. and Torsvik, T.H. 2012. Absolute plate motions in a reference frame defined by moving hot spots in the Pacific, Atlantic, and Indian oceans. *Journal of Geophysical Research: Solid Earth*, **117**, https://doi.org/10.1029/2011jb009072.
Eichelberger, N. and McQuarrie, N. 2015. Kinematic reconstruction of the Bolivian orocline. *Geosphere*, **11**, 445-462.
Engebretson, D.C., Cox, A. and Gordon, R.G. 1985. Relative motions between oceanic plates of the Pacific basin. *Journal of Geophysical Research*, **89**, 10291-10310.
England, P.C. and Thompson, A.B. 1984. Pressure—temperature—time paths of regional metamorphism I. Heat transfer during the evolution of regions of thickened continental crust. *Journal of Petrology*, **25**, 894-928.
Eyles, N., Eyles, C.H. and Miall, A.D. 1983. Lithofacies types and vertical profile models; an alternative approach to the description and environmental interpretation of glacial diamict and diamictite sequences. *Sedimentology*, **30**, 393-410.
Faccenna, C., Jolivet, L., Piromallo, C. and Morelli, A. 2003. Subduction and the depth of convection in the Mediterranean mantle. *Journal of Geophysical Research: Solid Earth*, **108**, https://doi.org/10.1029/2001jb001690.
Fu, R.R. and van Hinsbergen, D.J.J. 2026. Paleomagnetism and tectonics: a user's guide. *In*: Webb, A.A.G., Briggs, S.M., Ganbat, A., Genge, M.C. and Moore, W.B. (eds) *Methods in Tectonics. Geological Society, London, Geoscience in Practice*.
Fuston, S. and Wu, J. 2021. Raising the Resurrection plate from an unfolded-slab plate tectonic reconstruction of northwestern North America since early Cenozoic time. *Geological Society of America Bulletin*, **133**, 1128-1140.
Fyhn, M.B.W., Boldreel, L.O. and Nielsen, L.H. 2010. Escape tectonism in the Gulf of Thailand: Paleogene left-lateral pull-apart rifting in the Vietnamese part of the Malay Basin. *Tectonophysics*, **483**, 365-376, https://doi.org/10.1016/j.tecto.2009.11.004.

Gaastra, K.M., Gordon, R.G. and Woodworth, D.T. 2022. Quantification of Pacific Plate Hotspot Tracks Since 80 Ma. *Tectonics*, **41**, e2021TC006772.
García-Casco, A., Iturralde-Vinent, M.A. and Pindell, J. 2008. Latest Cretaceous Collision/Accretion between the Caribbean Plate and Caribeana: Origin of Metamorphic Terranes in the Greater Antilles. *International Geology Review*, **50**, 781-809, https://doi.org/10.2747/0020-6814.50.9.781.
Garnero, E.J. 2000. Heterogeneity of the lowermost mantle. *Annual Review of Earth and Planetary Sciences*, **28**, 509-537.
Gartrell, A., Keep, M., van der Riet, C., Paterniti, L., Ban, S. and Lang, S. 2022. Hyperextension and polyphase rifting: Impact on inversion tectonics and stratigraphic architecture of the North West Shelf, Australia. *Marine and Petroleum Geology*, **139**, 105594.
Glazner, A.F. and Bartley, J.M. 1985. Evolution of lithospheric strength after thrusting. *Geology*, **13**, 42-45.
Goes, S., Agrusta, R., van Hunen, J. and Garel, F. 2017. Subduction-transition zone interaction: A review. *Geosphere*, **13**, 644-664.
Goldreich, P. and Toomre, A. 1969. Some remarks on polar wandering. *Journal of Geophysical Research*, **74**, 2555-2567, https://doi.org/10.1029/JB074i010p02555.
Golombek, M.P. and Phillips, R.J. 2010. Mars tectonics. *Planetary tectonics*, **11**, 183-232.
Gradstein, F.M., Ogg, J.G., Schmitz, M.D. and Ogg, G.M. 2020. *Geologic time scale 2020*. Elsevier.
Grand, S.P., Van der Hilst, R.D. and Widiyantoro, S. 1997. High resolution global tomography: a snapshot of convection in the Earth. *Geological Society of America Today*, **7**.
Greenough, J.D., Kamo, S.L., Davis, D.W., Larson, K., Zhang, Z., Layton-Matthews, D., De Vera, J. and Bergquist, B.A. 2021. Old subcontinental mantle zircon below Oahu. *Communications Earth & Environment*, **2**, 189.
Guilmette, C., Smit, M.A., van Hinsbergen, D.J.J., Gürer, D., Corfu, F., Charette, B., Maffione, M., Rabeau, O. and Savard, D. 2018. Forced subduction initiation recorded in the sole and crust of the Semail Ophiolite of Oman. *Nature Geoscience*, **11**, 688-695.
Guilmette, C., van Hinsbergen, D.J.J., Smit, M.A., Godet, A., Fournier-Roy, F., Butler, J.P., Maffione, M., Li, S. and Hodges, K. 2023. Formation of the Xigaze Metamorphic Sole under Tibetan continental lithosphere reveals generic characteristics of subduction initiation. *Communications Earth & Environment*, **4**, 339.
Hacker, B.R. 1991. The role of deformation in the formation of metamorphic gradients: ridge subduction beneath the Oman ophiolite. *Tectonics*, **10**, 455-473.
Hacker, B.R. 1994. Rapid emplacement of young oceanic lithosphere: argon geochronology of the Oman ophiolite. *Science*, **265**, 1563-1565.
Hafkenscheid, E., Wortel, M.J.R. and Spakman, W. 2006. Subduction history of the Tethyan region derived from seismic tomography and tectonic reconstructions. *Journal of Geophysical Research*, **111**, https://doi.org/10.1029/2005jb003791.
Hagstrum, J.T. and Sedlock, R.L. 1992. Paleomagnetism of Mesozoic red chert from Cedros Island and the San Benito Islands, Baja California, Mexico revisited. *Geophysical Research Letters*, **19**, 329-332.

Hall, C.E., Gurnis, M., Sdrolias, M., Lavier, L.L. and Müller, R.D. 2003. Catastrophic initiation of subduction following forced convergence across fracture zones. *Earth and Planetary Science Letters*, **212**, 15-30, https://doi.org/10.1016/s0012-821x(03)00242-5.
Handy, M.R., Schmid, S.M., Bousquet, R., Kissling, E. and Bernoulli, D. 2010. Reconciling plate-tectonic reconstructions of Alpine Tethys with the geological–geophysical record of spreading and subduction in the Alps. *Earth-Science Reviews*, **102**, 121-158.
Hauck II, S.A., Dombard, A.J., Phillips, R.J. and Solomon, S.C. 2004. Internal and tectonic evolution of Mercury. *Earth and Planetary Science Letters*, **222**, 713-728.
Hu, X., Garzanti, E., Wang, J., Huang, W., An, W. and Webb, A. 2016. The timing of India-Asia collision onset – Facts, theories, controversies. *Earth-Science Reviews*, **160**, 264-299, https://doi.org/10.1016/j.earscirev.2016.07.014.
Inwood, J., Morris, A., Anderson, M.W. and Robertson, A.H.F. 2009. Neotethyan intraoceanic microplate rotation and variations in spreading axis orientation: Palaeomagnetic evidence from the Hatay ophiolite (southern Turkey). *Earth and Planetary Science Letters*, **280**, 105-117, https://doi.org/10.1016/j.epsl.2009.01.021.
Isozaki, Y., Maruyama, S. and Furuoka, F. 1990. Accreted oceanic materials in Japan. *Tectonophysics*, **181**, 179-205.
Isozaki, Y., Aoki, K., Nakama, T. and Yanai, S. 2010. New insight into a subduction-related orogen: A reappraisal of the geotectonic framework and evolution of the Japanese Islands. *Gondwana Research*, **18**, 82-105, https://doi.org/10.1016/j.gr.2010.02.015.
Jamieson, R.A. 1986. P-T paths from high temperature shear zones beneath ophiolites. *Journal of Metamorphic Geology*, **4**, 3-22.
Johnston, S.T. 2001. The Great Alaskan Terrane Wreck: reconciliation of paleomagnetic and geological data in the northern Cordillera. *Earth and Planetary Science Letters*, **193**, 259-272.
Jolivet, L., Faccenna, C., Goffé, B., Burov, E. and Agard, P. 2003. Subduction tectonics and exhumation of high-pressure metamorphic rocks in the Mediterranean orogens. *American Journal of Science*, **303**, 353-409.
Kapp, P. and DeCelles, P.G. 2019. Mesozoic–Cenozoic geological evolution of the Himalayan-Tibetan orogen and working tectonic hypotheses. *American Journal of Science*, **319**, 159-254.
Kimbrough, D.L. and Moore, T.E. 2003. Ophiolite and volcanic arc assemblages on the Vizcaino Peninsula and Cedros Island, Baja California Sur, Mexico: Mesozoic forearc lithosphere of the Cordilleran magmatic arc. *SPECIAL PAPERS-GEOLOGICAL SOCIETY OF AMERICA*, 43-72.
Kissel, C. and Laj, C. 1988. The Tertiary geodynamical evolution of the Aegean arc: a paleomagnetic reconstruction. *Tectonophysics*, **146**, 183-201.
Kotowski, A., Seyler, C.E., Kirkpatrick, J.D. and van Hinsbergen, D.J.J. 2025. Coupled mineral-mechanical changes during plate interface cooling may explain catastrophic subduction initiation. *Journal of Geophysical Research*, **in press**.
Kotowski, A.J., Cloos, M., Stockli, D.F. and Bos Orent, E. 2021. Structural and thermal evolution of an infant subduction shear zone: Insights from sub-ophiolite metamorphic rocks recovered from Oman Drilling Project Site BT-1B. *Journal of Geophysical Research: Solid Earth*, **126**, e2021JB021702.

Kreemer, C., Holt, W.E. and Haines, A.J. 2003. An integrated global model of present-day plate motions and plate boundary deformation. *Geophysical Journal International*, **154**, 8-34.
Kreemer, C., Blewitt, G. and Klein, E.C. 2014. A geodetic plate motion and Global Strain Rate Model. *Geochemistry, Geophysics, Geosystems*, **15**, 3849-3889.
Lallemand, S. and Arcay, D. 2021. Subduction initiation from the earliest stages to self-sustained subduction: Insights from the analysis of 70 Cenozoic sites. *Earth-Science Reviews*, **221**, 103779.
Lázaro, C., Blanco-Quintero, I.F., Rojas-Agramonte, Y., Proenza, J.A., Núñez-Cambra, K. and García-Casco, A. 2013. First description of a metamorphic sole related to ophiolite obduction in the northern Caribbean: Geochemistry and petrology of the Güira de Jauco Amphibolite complex (eastern Cuba) and tectonic implications. *Lithos*, **179**, 193-210, https://doi.org/10.1016/j.lithos.2013.08.019.
Leloup, P.H., Lacassin, R., Tapponnier, P., Schärer, U., Zhong, D., Liu, X., Zhang, L., Ji, S. and Trinh, P.T. 1995. The Ailao Shan-Red river shear zone (Yunnan, China), tertiary transform boundary of Indochina. *Tectonophysics*, **251**, 3-84.
Leng, W. and Gurnis, M. 2011. Dynamics of subduction initiation with different evolutionary pathways. *Geochemistry, Geophysics, Geosystems*, **12**, n/a-n/a, https://doi.org/10.1029/2011gc003877.
Li, S., Advokaat, E.L., van Hinsbergen, D.J.J., Koymans, M., Deng, C. and Zhu, R. 2017. Paleomagnetic constraints on the Mesozoic-Cenozoic paleolatitudinal and rotational history of Indochina and South China: Review and updated kinematic reconstruction. *Earth-Science Reviews*, **171**, 58-77, https://doi.org/10.1016/j.earscirev.2017.05.007.
Liu, C.-Z., Dick, H.J., Mitchell, R.N., Wei, W., Zhang, Z.-Y., Hofmann, A.W., Yang, J.-F. and Li, Y. 2022. Archean cratonic mantle recycled at a mid-ocean ridge. *Science Advances*, **8**, eabn6749.
Liu, L., Spasojevic, S. and Gurnis, M. 2008. Reconstructing Farallon plate subduction beneath North America back to the Late Cretaceous. *Science*, **322**, 934-938.
Liu, L., Shi, D. and Klemperer, S.L. 2025. The Indian Plate subducting below the Tibet Plateau is tearing apart. *Communications Earth & Environment*, **6**, 616.
Lonsdale, P. 2005. Creation of the Cocos and Nazca plates by fission of the Farallon plate. *Tectonophysics*, **404**, 237-264.
Macgregor, D. 2015. History of the development of the East African Rift System: A series of interpreted maps through time. *Journal of African Earth Sciences*, **101**, 232-252.
Maffione, M. and van Hinsbergen, D.J.J. 2018. Reconstructing plate boundaries in the Jurassic Neo-Tethys from the East and West Vardar Ophiolites (Greece, Serbia). *Tectonics*, https://doi.org/10.1002/2017tc004790.
Maffione, M., van Hinsbergen, D.J.J., de Gelder, G.I.N.O., van der Goes, F.C. and Morris, A. 2017. Kinematics of Late Cretaceous subduction initiation in the Neo-Tethys Ocean reconstructed from ophiolites of Turkey, Cyprus, and Syria. *Journal of Geophysical Research: Solid Earth*, **122**, 3953-3976, https://doi.org/10.1002/2016jb013821.
Maffione, M., Thieulot, C., van Hinsbergen, D.J.J., Morris, A., Plümper, O. and Spakman, W. 2015. Dynamics of intraoceanic subduction initiation: 1. Oceanic detachment fault

inversion and the formation of supra-subduction zone ophiolites. *Geochemistry, Geophysics, Geosystems*, **16**, 1753-1770, https://doi.org/10.1002/2015gc005746.
Man, B., Rothery, D.A., Balme, M.R., Conway, S.J. and Wright, J. 2023. Widespread small grabens consistent with recent tectonism on Mercury. *Nature Geoscience*, **16**, 856-862.
Maremmani, A., van Hinsbergen, D.J., Advokaat, E.L., Kotowski, A.J. and Guilmette, C. 2025. Orogenic architecture diagrams to reconstruct paleogeography and plate tectonics: Newfoundland (Canada) as a case study. *Journal of the Geological Society of London*, **in press**.
Martin, C.R., Jagoutz, O., Upadhyay, R., Royden, L.H., Eddy, M.P., Bailey, E., Nichols, C.I. and Weiss, B.P. 2020. Paleocene latitude of the Kohistan–Ladakh arc indicates multistage India–Eurasia collision. *Proceedings of the National Academy of Sciences*, **117**, 29487-29494.
McKenzie, D.P. and Parker, R.L. 1967. The North Pacific: an example of tectonics on a sphere. *Nature*, **216**, 1276-1280.
McNamara, A.K. 2019. A review of large low shear velocity provinces and ultra low velocity zones. *Tectonophysics*, **760**, 199-220.
McQuarrie, N. and Wernicke, B.P. 2005. An animated tectonic reconstruction of southwestern North America since 36 Ma. *Geosphere*, **1**, 147-172, https://doi.org/10.1130/ges00016.1.
McQuarrie, N. and van Hinsbergen, D.J.J. 2013. Retrodeforming the Arabia-Eurasia collision zone: Age of collision versus magnitude of continental subduction. *Geology*, **41**, 315-318, https://doi.org/10.1130/g33591.1.
Merdith, A.S., Williams, S.E., Collins, A.S., Tetley, M.G., Mulder, J.A., Blades, M.L., Young, A., Armistead, S.E., Cannon, J. and Zahirovic, S. 2021. Extending full-plate tectonic models into deep time: Linking the neoproterozoic and the phanerozoic. *Earth-Science Reviews*, **214**, 103477.
Miller, M., Gorbatov, A. and Kennett, B. 2005. Heterogeneity within the subducting Pacific slab beneath the Izu–Bonin–Mariana arc: Evidence from tomography using 3D ray tracing inversion techniques. *Earth and Planetary Science Letters*, **235**, 331-342, https://doi.org/10.1016/j.epsl.2005.04.007.
Miyashiro, A. 1973. The Troodos ophiolitic complex was probably formed in an island arc. *Earth and Planetary Science Letters*, **19**, 218-224.
Montheil, L., van Hinsbergen, D.J.J., Philippon, M., Boschman, L.M., Cornée, J.J., Audemard, F., Wessels, R., Leroy, S., Roncal, J. and Münch, P. 2025. Caribbean biodiversity shaped by subduction zone processes along the Lesser Antilles arch. *Communications Earth and Environment*.
Morgan, W.J. 1971. Convection plumes in the lower mantle. *Nature*, **230**, 42.
Mortimer, N. 2004. New Zealand's Geological Foundations. *Gondwana Research*, **7**, 261-272, https://doi.org/10.1016/s1342-937x(05)70324-5.
Mulcahy, S.R., Starnes, J.K., Day, H.W., Coble, M.A. and Vervoort, J.D. 2018. Early onset of Franciscan subduction. *Tectonics*, **37**, 1194-1209.

Müller, R.D., Royer, J.-Y. and Lawver, L.A. 1993. Revised plate motions relative to the hotspots from combined Atlantic and Indian Ocean hotspot tracks. *Geology*, **21**, 275-278.
Müller, R.D., Roest, W.R. and Royer, J.-Y. 1998. Asymmetric sea-floor spreading caused by ridge–plume interactions. *Nature*, **396**, 455-459.
Müller, R.D., Cannon, J., Tetley, M., Williams, S.E., Cao, X., Flament, N., Bodur, Ö.F., Zahirovic, S. and Merdith, A. 2022. A tectonic-rules based mantle reference frame since 1 billion years ago–implications for supercontinent cycles and plate-mantle system evolution. *Solid Earth*, **13**, 1127-1159.
Müller, R.D., Cannon, J., Qin, X., Watson, R.J., Gurnis, M., Williams, S., Pfaffelmoser, T., Seton, M., Russell, S.H. and Zahirovic, S. 2018. GPlates: building a virtual Earth through deep time. *Geochemistry, Geophysics, Geosystems*, **19**, 2243-2261.
Müller, R.D., Zahirovic, S., Williams, S.E., Cannon, J., Seton, M., Bower, D.J., Tetley, M.G., Heine, C., Le Breton, E. and Liu, S. 2019. A global plate model including lithospheric deformation along major rifts and orogens since the Triassic. *Tectonics*.
Nahm, A.L., Watters, T.R., Johnson, C.L., Banks, M.E., van der Bogert, C.H., Weber, R.C. and Andrews-Hanna, J.C. 2023. Tectonics of the Moon. *Reviews in Mineralogy and Geochemistry*, **89**, 691-727.
Nimmo, F. and McKenzie, D. 1998. Volcanism and tectonics on Venus. *Annual Review of Earth and Planetary Sciences*, **26**, 23-51.
Nimmo, F. and Stevenson, D. 2000. Influence of early plate tectonics on the thermal evolution and magnetic field of Mars. *Journal of Geophysical Research: Planets*, **105**, 11969-11979.
Nolet, G., Allen, R. and Zhao, D. 2007. Mantle plume tomography. *Chemical Geology*, **241**, 248-263.
O'Neill, C., Müller, D. and Steinberger, B. 2005. On the uncertainties in hot spot reconstructions and the significance of moving hot spot reference frames. *Geochemistry, Geophysics, Geosystems*, **6**, n/a-n/a, https://doi.org/10.1029/2004gc000784.
Oda, H. and Suzuki, H. 2000. Paleomagnetism of Triassic and Jurassic red bedded chert of the Inuyama area, central Japan. *Journal of Geophysical Research: Solid Earth*, **105**, 25743-25767.
Palin, R.M. and Santosh, M. 2021. Plate tectonics: What, where, why, and when? *Gondwana Research*, **100**, 3-24, https://doi.org/10.1016/j.gr.2020.11.001.
Pearce, J.A., Lippard, S. and Roberts, S. 1984. Characteristics and tectonic significance of supra-subduction zone ophiolites. *Geological Society, London, Special Publications*, **16**, 77-94.
Peters, K., Plunder, A., Guilmette, C., Brouwer, F.M., Kuiper, K.F., Wijbrans, J., Van Roermund, H.L.M., van Elsas, R., Gerretsen, H., Hupkes, J., Maffione, M. and van Hinsbergen, D.J.J. 2026. The Pınarbaşı metamorphic sole (Turkey) as a geological archive of subduction initiation in the Cretaceous Neotethys Ocean. *Tektonika*, **submitted**.

Peters, T. and Mercolli, I. 1998. Extremely thin oceanic crust in the Proto-Indian Ocean: Evidence from the Masirah Ophiolite, Sultanate of Oman. *Journal of Geophysical Research: Solid Earth*, **103**, 677-689, https://doi.org/10.1029/97jb02674.

Phillips-Lander, C.M. and Dilek, Y. 2009. Structural architecture of the sheeted dike complex and extensional tectonics of the Jurassic Mirdita ophiolite, Albania. *Lithos*, **108**, 192-206.

Pilot, J., Werner, C.-D., Haubrich, F. and Baumann, N. 1998. Palaeozoic and proterozoic zircons from the Mid-Atlantic ridge. *Nature*, **393**, 676.

Platt, J. 1986. Dynamics of orogenic wedges and the uplift of high-pressure metamorphic rocks. *Geological Society of America Bulletin*, **97**, 1037-1053.

Plunder, A., Bandyopadhyay, D., Ganerød, M., Advokaat, E.L., Ghosh, B., Bandopadhyay, P. and van Hinsbergen, D.J.J. 2020. History of subduction polarity reversal during arc-continent collision: constraints from the Andaman Ophiolite and its metamorphic sole. *Tectonics*, e2019TC005762.

Pourteau, A., Scherer, E.E., Schorn, S., Bast, R., Schmidt, A. and Ebert, L. 2019. Thermal evolution of an ancient subduction interface revealed by Lu–Hf garnet geochronology, Halilbağı Complex (Anatolia). *Geoscience Frontiers*, **10**, 127-148, https://doi.org/10.1016/j.gsf.2018.03.004.

Reagan, M.K., McClelland, W.C., Girard, G., Goff, K.R., Peate, D.W., Ohara, Y. and Stern, R.J. 2013. The geology of the southern Mariana fore-arc crust: Implications for the scale of Eocene volcanism in the western Pacific. *Earth and Planetary Science Letters*, **380**, 41-51, https://doi.org/10.1016/j.epsl.2013.08.013.

Replumaz, A. and Tapponnier, P. 2003. Reconstruction of the deformed collision zone Between India and Asia by backward motion of lithospheric blocks. *Journal of Geophysical Research: Solid Earth*, **108**, https://doi.org/10.1029/2001jb000661.

Reston, T.J. 2005. Polyphase faulting during the development of the west Galicia rifted margin. *Earth and Planetary Science Letters*, **237**, 561-576.

Ribe, N.M. and al., e. 2007. Buckling instabilities of subducted lithosphere beneath the transition zone. *Earth and Planetary Science Letters*, **254**, 173–179.

Richter, M., Nebel, O., Maas, R., Mather, B., Nebel-Jacobsen, Y., Capitanio, F.A., Dick, H.J. and Cawood, P.A. 2020. An Early Cretaceous subduction-modified mantle underneath the ultraslow spreading Gakkel Ridge, Arctic Ocean. *Science Advances*, **6**, eabb4340.

Rioux, M., Garber, J., Bauer, A., Bowring, S., Searle, M., Kelemen, P. and Hacker, B. 2016. Synchronous formation of the metamorphic sole and igneous crust of the Semail ophiolite: New constraints on the tectonic evolution during ophiolite formation from high-precision U–Pb zircon geochronology. *Earth and Planetary Science Letters*, **451**, 185-195.

Robinson, P.T., Malpas, J., Dilek, Y. and Zhou, M. 2008. The significance of sheeted dike complexes in ophiolites. *GSA Today*, **18**, 4-10.

Rojas-Agramonte, Y., Pardo, N., van Hinsbergen, D.J.J., Marroquín-Gómez, M.P., Gerdes, A., Winter, C., Albert, R., Liu, S. and García-Casco, A. 2024. Zircon xenocrysts from Easter Island (Rapa Nui) reveal hotspot activity since the middle Jurassic. *AGU Advances*, **5**, e2024AV001351, https://doi.org/https://doi.org/10.1029/2024AV001351.

Rojas-Agramonte, Y., Kaus, B.J., Piccolo, A., Williams, I.S., Gerdes, A., Wong, J., Xie, H., Buhre, S., Toulkeridis, T. and Montero, P. 2022. Zircon Dates Long-Lived Plume Dynamics in Oceanic Islands. *Geochemistry, Geophysics, Geosystems*, **23**, e2022GC010485.

Rossetti, F., Goffé, B., Monié, P., Faccenna, C. and Vignaroli, G. 2004. Alpine orogenic P-T-t-deformation history of the Catena Costiera area and surrounding regions (Calabrian Arc, southern Italy): The nappe edifice of north Calabria revised with insights on the Tyrrhenian-Apennine system formation. *Tectonics*, **23**, n/a-n/a, https://doi.org/10.1029/2003tc001560.

Schellart, W.P. 2008. Subduction zone trench migration: Slab driven or overriding-plate-driven? *Physics of the Earth and Planetary Interiors*, **170**, 73-88, https://doi.org/10.1016/j.pepi.2008.07.040.

Schepers, G., van Hinsbergen, D.J.J., Spakman, W., Kosters, M.E., Boschman, L.M. and McQuarrie, N. 2017. South-American plate advance and forced Andean trench retreat as drivers for transient flat subduction episodes. *Nat Commun*, **8**, 15249, https://doi.org/10.1038/ncomms15249.

Schoenfeld, A.M. and Yin, A. 2024. Quantifying tidal versus non-tidal stresses in driving time-varying fluxes of Enceladus' plume eruptions. *Icarus*, **415**, 116064.

Schouten, T.L., Gebraad, L., Noe, S., Gülcher, A.J., Thrastarson, S., van Herwaarden, D.-P. and Fichtner, A. 2024. Full-waveform inversion reveals diverse origins of lower mantle positive wave speed anomalies. *Scientific Reports*, **14**, 26708.

Searle, M.P. 2006. Role of the Red River Shear zone, Yunnan and Vietnam, in the continental extrusion of SE Asia. *Journal of the Geological Society*, **163**, 1025-1036, https://doi.org/10.1144/0016-76492005-144.

Searle, M.P. and Cox, J.O.N. 2002. Subduction zone metamorphism during formation and emplacement of the Semail ophiolite in the Oman Mountains. *Geological Magazine*, **139**, https://doi.org/10.1017/s0016756802006532.

Senkans, A., Leroy, S., d'Acremont, E., Castilla, R. and Despinois, F. 2019. Polyphase rifting and break-up of the central Mozambique margin. *Marine and Petroleum Geology*, **100**, 412-433.

Seton, M., Williams, S.E., Domeier, M., Collins, A.S. and Sigloch, K. 2023. Deconstructing plate tectonic reconstructions. *Nature Reviews Earth & Environment*, **4**, 185-204.

Seton, M., Müller, R.D., Zahirovic, S., Gaina, C., Torsvik, T., Shephard, G., Talsma, A., Gurnis, M., Turner, M., Maus, S. and Chandler, M. 2012. Global continental and ocean basin reconstructions since 200Ma. *Earth-Science Reviews*, **113**, 212-270, https://doi.org/10.1016/j.earscirev.2012.03.002.

Sigloch, K. and Mihalynuk, M.G. 2013. Intra-oceanic subduction shaped the assembly of Cordilleran North America. *Nature*, **496**, 50-56, https://doi.org/10.1038/nature12019.

Sigloch, K. and Mihalynuk, M.G. 2017. Mantle and geological evidence for a Late Jurassic–Cretaceous suture spanning North America. *GSA Bulletin*, **129**, 1489-1520, https://doi.org/10.1130/b31529.1.

Soret, M., Agard, P., Dubacq, B., Plunder, A. and Yamato, P. 2017. Petrological evidence for stepwise accretion of metamorphic soles during subduction infancy (Semail ophiolite,

Oman and UAE). *Journal of Metamorphic Geology*, **35**, 1051-1080, https://doi.org/10.1111/jmg.12267.
Spakman, W., Wortel, M. and Vlaar, N. 1988. The Hellenic subduction zone: a tomographic image and its geodynamic implications. *Geophysical Research Letters*, **15**, 60-63.
Steinberger, B. 2000. Plumes in a convecting mantle: Models and observations for individual hotspots. *Journal of Geophysical Research: Solid Earth*, **105**, 11127-11152.
Steinberger, B. and Torsvik, T.H. 2010. Toward an explanation for the present and past locations of the poles. *Geochemistry, Geophysics, Geosystems*, **11**, n/a-n/a, https://doi.org/10.1029/2009gc002889.
Stern, R.J. 1994. Arc assembly and continental collision in the Neoproterozoic East African Orogen: implications for the consolidation of Gondwanaland. *Annual Review of Earth and Planetary Sciences*, **22**, 319-351.
Stern, R.J. and Bloomer, S.H. 1992. Subduction zone infancy: Examples from the Eocene Izu-Bonin-Mariana and Jurassic California arcs. *Geological Society of America Bulletin*, **104**, 1621-1636, https://doi.org/10.1130/0016-7606(1992)104<1621:Szieft>2.3.Co;2.
Stern, R.J., Reagan, M., Ishizuka, O., Ohara, Y. and Whattam, S. 2012. To understand subduction initiation, study forearc crust: To understand forearc crust, study ophiolites. *Lithosphere*, **4**, 469-483, https://doi.org/10.1130/l183.1.
Stracke, A., Willig, M., Genske, F., Béguelin, P. and Todd, E. 2022. Chemical geodynamics insights from a machine learning approach. *Geochemistry, Geophysics, Geosystems*, e2022GC010606.
Talavera-Soza, S., Cobden, L., Faul, U.H. and Deuss, A. 2025. Global 3D model of mantle attenuation using seismic normal modes. *Nature*, **637**, 1131-1135.
Tarduno, J.A., McWilliams, M., Debiche, M.G., Sliter, W.V. and Blake, M. 1985. Franciscan Complex Calera limestones: Accreted remnants of Farallon plate oceanic plateaus. *Nature*, **317**, 345-347.
Tarduno, J.A., McWilliams, M., Sliter, W.V., Cook, H.E., Blake Jr, M.C. and Premoli-Silva, I. 1986. Southern hemisphere origin of the Cretaceous Laytonville Limestone of California. *Science*, **231**, 1425-1428.
Tetley, M.G., Williams, S.E., Gurnis, M., Flament, N. and Müller, R.D. 2019. Constraining absolute plate motions since the Triassic. *Journal of Geophysical Research: Solid Earth*, **124**, 7231-7258.
Topuz, G., Celik, O.F., Şengör, A.M.C., Altintas, I.E., Zack, T., Rolland, Y. and Barth, M. 2014. Jurassic ophiolite formation and emplacement as backstop to a subduction-accretion complex in northeast Turkey, the Refahiye ophiolite, and relation to the Balkan ophiolites. *American Journal of Science*, **313**, 1054-1087, https://doi.org/10.2475/10.2013.04.
Torsvik, T.H. and Cocks, L.R.M. 2017. *Earth history and palaeogeography*. Cambridge University Press.
Torsvik, T.H., Müller, R.D., Van der Voo, R., Steinberger, B. and Gaina, C. 2008. Global plate motion frames: Toward a unified model. *Reviews of Geophysics*, **46**, https://doi.org/10.1029/2007rg000227.

Torsvik, T.H., Burke, K., Steinberger, B., Webb, S.J. and Ashwal, L.D. 2010. Diamonds sampled by plumes from the core-mantle boundary. *Nature*, **466**, 352-355, https://doi.org/10.1038/nature09216.

Torsvik, T.H., Steinberger, B., Shephard, G.E., Doubrovine, P.V., Gaina, C., Domeier, M., Conrad, C.P. and Sager, W.W. 2019. Pacific-Panthalassic reconstructions: Overview, errata and the way forward. *Geochemistry, Geophysics, Geosystems*, **20**, 3659-3689.

Torsvik, T.H., van der Voo, R., Doubrovine, P.V., Burke, K., Steinberger, B., Ashwal, L.D., Tronnes, R.G., Webb, S.J. and Bull, A.L. 2014. Deep mantle structure as a reference frame for movements in and on the Earth. *Proc Natl Acad Sci U S A*, **111**, 8735-8740, https://doi.org/10.1073/pnas.1318135111.

Torsvik, T.H., Van der Voo, R., Preeden, U., Mac Niocaill, C., Steinberger, B., Doubrovine, P.V., van Hinsbergen, D.J.J., Domeier, M., Gaina, C., Tohver, E., Meert, J.G., McCausland, P.J.A. and Cocks, L.R.M. 2012. Phanerozoic polar wander, palaeogeography and dynamics. *Earth-Science Reviews*, **114**, 325-368, https://doi.org/10.1016/j.earscirev.2012.06.007.

Ueda, H. 2006. Hokkaido. *In*: Moreno, T., Wallis, S., Kojima, T. and Gibbons, W. (eds) *The geology of Japan*. Geological Society, Geology of Series, London, England, 201-221.

Urann, B., Dick, H., Parnell-Turner, R. and Casey, J. 2020. Recycled arc mantle recovered from the Mid-Atlantic Ridge. *Nature Communications*, **11**, 1-9.

Vaes, B. and van Hinsbergen, D.J.J. 2025. Slow true polar wander around varying equatorial axes since 320 Ma. *AGU Advances*, **6**, e2024AV001515.

Vaes, B., van Hinsbergen, D.J.J., van de Lagemaat, S.H.A., van der Wiel, E., Lom, N., Advokaat, E., Boschman, L.M., Gallo, L.C., Greve, A., Guilmette, C., Li, S., Lippert, P.C., Montheil, L., Qayyum, A. and Langereis, C.G. 2023. A global apparent polar wander path for the last 320 Ma calculated from site-level paleomagnetic data. *Earth-Science Reviews*, **245**, 104547, https://doi.org/https://doi.org/10.31223/X55368.

van de Lagemaat, S.H., Cao, L., Asis, J., Advokaat, E., Mason, P., Dekkers, M.J. and van Hinsbergen, D.J.J. 2024. Causes of Late Cretaceous subduction termination below South China and Borneo: Was the Proto-South China Sea underlain by an oceanic plateau? *Geoscience Frontiers*, **15**, 101752.

van de Lagemaat, S.H.A. and van Hinsbergen, D.J.J. 2024. Plate tectonic cross-roads: Reconstructing the Panthalassa-Neotethys Junction Region from Philippine Sea Plate and Australasian oceans and orogens. *Gondwana Research*, **126**, 129-201, https://doi.org/https://doi.org/10.1016/j.gr.2023.09.013.

van de Lagemaat, S.H.A., Kamp, P.J., Boschman, L.M. and van Hinsbergen, D.J.J. 2023. Reconciling the Cretaceous breakup and demise of the Phoenix Plate with East Gondwana orogenesis in New Zealand. *Earth-Science Reviews*, **236**, 104276.

van der Hist, R., Engdahl, R., Spakman, W. and Nolet, G. 1991. Tomographic imaging of subducted lithosphere below northwest Pacific island arcs. *Nature*, **353**, 37-43.

van der Meer, D.G., van Hinsbergen, D.J.J. and Spakman, W. 2018. Atlas of the underworld: Slab remnants in the mantle, their sinking history, and a new outlook on lower mantle viscosity. *Tectonophysics*, **723**, 309-448, https://doi.org/10.1016/j.tecto.2017.10.004.

van der Meer, D.G., Spakman, W., van Hinsbergen, D.J.J., Amaru, M.L. and Torsvik, T.H. 2010. Towards absolute plate motions constrained by lower-mantle slab remnants. *Nature Geoscience*, **3**, 36-40, https://doi.org/10.1038/ngeo708.

van der Meer, D.G., Torsvik, T.H., Spakman, W., van Hinsbergen, D.J.J. and Amaru, M.L. 2012. Intra-Panthalassa Ocean subduction zones revealed by fossil arcs and mantle structure. *Nature Geoscience*, **5**, 215-219, https://doi.org/10.1038/ngeo1401.

van der Meer, D.G., Zeebe, R.E., van Hinsbergen, D.J.J., Sluijs, A., Spakman, W. and Torsvik, T.H. 2014. Plate tectonic controls on atmospheric CO2 levels since the Triassic. *Proc Natl Acad Sci U S A*, **111**, 4380-4385, https://doi.org/10.1073/pnas.1315657111.

Van der Voo, R., Spakman, W. and Bijwaard, H. 1999a. Tethyan subducted slabs under India. *Earth and Planetary Science Letters*, **171**, 7-20.

Van der Voo, R., Spakman, W. and Bijwaard, H. 1999b. Mesozoic subducted slabs under Siberia. *Nature*, **397**, 246-249.

van der Wiel, E., van Hinsbergen, D.J.J., Thieulot, C. and Spakman, W. 2024a. Linking rates of slab sinking to long-term lower mantle flow and mixing. *Earth and Planetary Science Letters*, **625**, 118471.

van der Wiel, E., Pokorný, J., Čížková, H., Spakman, W., van den Berg, A.P. and van Hinsbergen, D.J. 2024b. Slab buckling as a driver for rapid oscillations in Indian plate motion and subduction rate. *Communications Earth & Environment*, **5**, 316.

van Hinsbergen, D.J.J. 2022. Indian Plate paleogeography, subduction, and horizontal underthrusting below Tibet: paradoxes, controvercies, and opportunities. *National Science Review*, **9**, nwac074, https://doi.org/https://doi.org/10.31223/X54M0V.

van Hinsbergen, D.J.J. and Schmid, S.M. 2012. Map view restoration of Aegean-West Anatolian accretion and extension since the Eocene. *Tectonics*, **31**, doi: 10.1029/2012tc003132, https://doi.org/10.1029/2012tc003132.

van Hinsbergen, D.J.J. and Schouten, T.L.A. 2021. Deciphering paleogeography from orogenic architecture: constructing orogens in a future supercontinent as thought experiment. *American Journal of Science*, **321**, 955-1031, https://doi.org/DOI 10.2475/06.2021.09.

van Hinsbergen, D.J.J., Lamont, T.N. and Guilmette, C. 2025. Lithospheric unzipping explaining hot orogenesis during continental subduction. *Tectonics*, **44**, e2025TC008993.

van Hinsbergen, D.J.J., Hafkenscheid, E., Spakman, W., Meulenkamp, J.E. and Wortel, R. 2005. Nappe stacking resulting from subduction of oceanic and continental lithosphere below Greece. *Geology*, **33**, https://doi.org/10.1130/g20878.1.

van Hinsbergen, D.J.J., Kapp, P., Dupont-Nivet, G., Lippert, P.C., DeCelles, P.G. and Torsvik, T.H. 2011. Restoration of Cenozoic deformation in Asia and the size of Greater India. *Tectonics*, **30**, n/a-n/a, https://doi.org/10.1029/2011tc002908.

van Hinsbergen, D.J.J., Spakman, W., de Boorder, H., van Dongen, M., Jowitt, S.M. and Mason, P.R. 2020a. Arc-type magmatism due to continental-edge plowing through ancient subduction-enriched mantle. *Geophysical Research Letters*, **47**, e2020GL087484.

van Hinsbergen, D.J.J., de Groot, L.V., van Schaik, S.J., Spakman, W., Bijl, P.K., Sluijs, A., Langereis, C.G. and Brinkhuis, H. 2015a. A Paleolatitude Calculator for Paleoclimate Studies. *PLoS One*, **10**, e0126946, https://doi.org/10.1371/journal.pone.0126946.

van Hinsbergen, D.J.J., Torsvik, T., Schmid, S.M., Matenco, L., Maffione, M., Vissers, R.L.M., Gürer, D. and Spakman, W. 2020b. Orogenic architecture of the Mediterranean region and kinematic reconstruction of its tectonic evolution since the Triassic. *Gondwana Research*, **81**, 79-229.

van Hinsbergen, D.J.J., Peters, K., Maffione, M., Spakman, W., Guilmette, C., Thieulot, C., Plümper, O., Gürer, D., Brouwer, F.M., Aldanmaz, E. and Kaymakcı, N. 2015b. Dynamics of intraoceanic subduction initiation: 2. Suprasubduction zone ophiolite formation and metamorphic sole exhumation in context of absolute plate motions. *Geochemistry, Geophysics, Geosystems*, **16**, 1771-1785, https://doi.org/10.1002/2015gc005745.

van Hinsbergen, D.J.J., Maffione, M., Plunder, A., Kaymakci, N., Ganerød, M., Hendriks, B.W.H., Corfu, F., Gürer, D., de Gelder, G.I.N.O., Peters, K., McPhee, P.J., Brouwer, F.M., Advokaat, E.L. and Vissers, R.L.M. 2016. Tectonic evolution and paleogeography of the Kırşehir Block and the Central Anatolian Ophiolites, Turkey. *Tectonics*, **35**, 983-1014, https://doi.org/10.1002/.

van Staal, C.R., Barr, S.M., Percival, J., Cook, F. and Clowes, R. 2012. Lithospheric architecture and tectonic evolution of the Canadian Appalachians and associated Atlantic margin. *Tectonic styles in Canada: The LITHOPROBE perspective: Geological Association of Canada Special Paper*, **49**, 41-95.

Vine, F.J. and Matthews, D.H. 1963. Magnetic anomalies over oceanic ridges. *Nature*, **199**, 947-949.

von Huene, R., Ranero, C.R. and Vannucchi, P. 2004. Generic model of subduction erosion. *Geology*, **32**, https://doi.org/10.1130/g20563.1.

Wagenaar, S.D.M., Vaes, B. and van Hinsbergen, D.J.J. 2025. Towards reconstructing mantle convection using a minimum-continent-motion mantle reference frame *Journal of Geophysical Research*, **in press**.

Wakabayashi, J. 2015. Anatomy of a subduction complex: architecture of the Franciscan Complex, California, at multiple length and time scales. *International Geology Review*, **57**, 669-746, https://doi.org/10.1080/00206814.2014.998728.

Wakabayashi, J. 2021. Field and petrographic reconnaissance of Franciscan complex rocks of Mount Diablo, California: Imbricated ocean floor stratigraphy with a roof exhumation fault system. *In*: Sullivan, R., Sloan, D., Unruh, J.R. and Schwartz, D.P. (eds) *Regional Geology of Mount Diablo, California: Its Tectonic Evolution on the North America Plate Boundary. Geological Society of America Memoirs*. https://doi.org/10.1130/2021.1217(09).

Watters, T.R. and Nimmo, F. 2010. The tectonics of Mercury. *Planetary tectonics*, **11**, 15.

Westerweel, J., Roperch, P., Licht, A., Dupont-Nivet, G., Win, Z., Poblete, F., Ruffet, G., Swe, H.H., Thi, M.K. and Aung, D.W. 2019. Burma Terrane part of the Trans-Tethyan arc during collision with India according to palaeomagnetic data. *Nature Geoscience*, **12**, 863-868.

Wolf, J. and Long, M.D. 2023. Lowermost mantle structure beneath the central Pacific Ocean: Ultralow velocity zones and seismic anisotropy. *Geochemistry, Geophysics, Geosystems*, **24**, e2022GC010853.
Woodward, N.B., Boyer, S.E. and Suppe, J. 1989. Balanced geological cross-sections. *Short course in geology*, **6**, 132.
Wu, J., Suppe, J., Lu, R. and Kanda, R. 2016. Philippine Sea and East Asian plate tectonics since 52 Ma constrained by new subducted slab reconstruction methods. *Journal of Geophysical Research: Solid Earth*, **121**, 4670-4741.
Wu, J., Lin, Y.-A., Flament, N., Wu, J.T.-J. and Liu, Y. 2022. Northwest Pacific-Izanagi plate tectonics since Cretaceous times from western Pacific mantle structure. *Earth and Planetary Science Letters*, **583**, 117445.
Wu, J.T.-J. and Wu, J. 2019. Izanagi-Pacific ridge subduction revealed by a 56 to 46 Ma magmatic gap along the northeast Asian margin. *Geology*, **47**, 953-957.
Wyld, S.J., Umhoefer, P.J., Wright, J.E., Haggart, J., Enkin, R. and Monger, J. 2006. Reconstructing northern Cordilleran terranes along known Cretaceous and Cenozoic strike-slip faults: Implications for the Baja British Columbia hypothesis and other models. *Paleogeography of the North American cordillera: Evidence for and against large-scale displacements: Geological Association of Canada Special Paper*, **46**, 277-298.
Yin, A. and Harrison, T.M. 2000. Geologic evolution of the Himalayan-Tibetan orogen. *Annual Review of Earth and Planetary Sciences*, **28**, 211-280.
Yin, A. and Pappalardo, R.T. 2015. Gravitational spreading, bookshelf faulting, and tectonic evolution of the South Polar Terrain of Saturn's moon Enceladus. *Icarus*, **260**, 409-439.
Yin, A., Nie, S., Craig, P., Harrison, T., Ryerson, F., Xianglin, Q. and Geng, Y. 1998. Late Cenozoic tectonic evolution of the southern Chinese Tian Shan. *Tectonics*, **17**, 1-27.
Yonkee, W.A. and Weil, A.B. 2015. Tectonic evolution of the Sevier and Laramide belts within the North American Cordillera orogenic system. *Earth-Science Reviews*, **150**, 531-593.
Zhao, D. 2007. Seismic images under 60 hotspots: Search for mantle plumes. *Gondwana Research*, **12**, 335-355.
Ziegler, P.A. and Cloetingh, S. 2004. Dynamic processes controlling evolution of rifted basins. *Earth-Science Reviews*, **64**, 1-50.